NASA CONTRACTOR REPORT 166589

(NASA-CR-166589-Pt-2) DOUBLE ARCH MIRROR STUDY. PART 2: ENGINEERING ANALYSIS REPORT Final Report, Apr. - May 1983 (Arizona Univ., Tucson.) 66 p HC AC4/MF A01 CSCL 13I G3/37

N84-31635

Unclas 20177

Double Arch Mirror Study
Part 2, Engineering Analysis Report

Bijan Iraninejad
Daniel Vukobratovich
University of Arizona

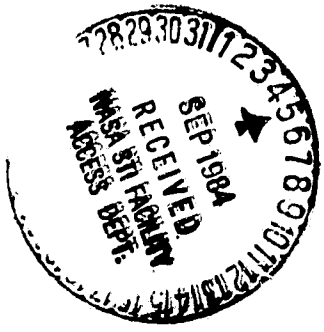

CONTRACT NAG2- 220
May 1983

NASA

NASA CONTRACTOR REPORT 166589

Double Arch Mirror Study
Part 2, Engineering Analysis Report

Bijan Iraninejad
Daniel Vukobratovich
University of Arizona
Optical Sciences Center

Prepared for
Ames Research Center
under Grant NAG2-220

National Aeronautics and
Space Administration

Ames Research Center
Moffett Field, California 94035

CONTENTS

1. INTRODUCTION 1

2. ANALYSIS 4

2.1. Force/Moment Transfer from Mount to Mirror 4
2.1.1. Cool Down, Zero Gravity 4
2.1.2. Cool Down, 1-G Loading 8
2.1.3. Temperature Effects 9

2.2. Stress in Flexures 14
2.2.1. Stress in Cryogenic Temperatures 14
2.2.2. Side Loading 15
2.2.3. Stress due to Mount Error 16
2.2.4. Critical Normal Stress 17

2.3. Influence of Mount on Figure Quality 17
2.3.1. Case I 20
2.3.2. Case II 27
2.3.3. Case III 27

3. FLEXURE DESIGN 30

3.1. Design Range 30
3.1.1. Manufacturing Requirements 30
3.1.2. Surface Quality Requirements 30
3.1.3. Stress Requirements 31

3.2. Design Calculations 32
3.2.1. 0-G Cool Down 32
3.2.2. 1-G Cool Down. Face Down Testing 32
3.2.3. Launch. Flexures in Tension 34
3.2.4. Emergency Landing. Flexures in Tension 34
3.2.5. Radial Tilt 34
3.2.6. Tangential Tilt 36
3.2.7. Flexure Error 36
3.2.8. Presence of Mount Error 37

4. STRESS IN THE MIRROR 39

5. CONCLUSION 47

REFERENCES 49

APPENDIX A 50

APPENDIX B 53

1. INTRODUCTION

The mount for the NASA Ames 20-in. double arch mirror must be designed to comply with the following requirements:

(1) The mirror will be assembled at room temperature (68°F) and used at cryogenic temperatures (-423°F). Therefore, the mount must provide a transition between the fused silica mirror and the aluminum base plate, without reducing the figure quality.

(2) The mirror will be cooled down and tested in a 1-G gravity field. Therefore, the mount must be designed not to reach its microyield stress in ground testing. The same criterion must be satisfied when the mirror is subjected to the launch load.

(3) The mount should be designed to survive emergency landing. In this case the survival is defined as developing stresses less than the yield stress. However, an attempt will be made to limit the emergency landing stresses to the microyield level.

(4) Realistic tolerances should be set for the manufacturing of the mount. The tightness of these tolerances will affect the figure quality. Furthermore, in light of the uncertainty about the magnitude and distribution of the internal stresses in the base plate, the effect of cryogenic temperatures on flatness of the plate cannot be predetermined. However, an acceptable design should allow for the manufacturing tolerances and the existence of tilt in the base plate and should minimize the sensitivity of figure quality to such factors.

(5) The mount should be designed to maintain the optical alignment of the mirror.

This study is subject to the following assumptions:

(1) The mirror is assumed to be very stiff. Generally speaking, this is a conservative assumption. A mirror with finite stiffness will result in lower stress in the flexures.

(2) The mirror material is Corning Code 7740 fused silica. The flexures are assumed to be made of titanium, 6Al-4V ELI, and the base plate as well as the dewar plate are assumed to be made of 6061 aluminum tooling plate. The assumed properties of these materials are given in Table 1.

Table 1. Material Properties

	Corning Code 7740	Titanium 6Al 4V ELI	6061 Aluminum Tooling Plate
Yield stress (psi)	--	240,000	42,000
Microyield stress (psi)	--	115,000	18,000
Modulus of elasticity (psi)	10×10^6	18×10^6	10.9×10^6
Poison ratio	0.17	0.33	0.33
Thermal contraction $\frac{L_T-L_{68}}{L_{68}}$	0	-175×10^{-5}	-420×10^{-5}

(3) Since the displacements in the mirror are small, it can be assumed that the induced moments and forces are decoupled. Therefore, deflection due to each component of a specific loading can be calculated independently and then, by using the principle of superposition, the deflections can be directly added to find the total deflection of the mirror.

(4) The range of deflections and stresses in the mirror and the base plate is well within the range of the elastic response. Therefore, once the figure quality is calculated for a specific loading, it can be multiplied by the proper scaling factors to give the figure quality for various magnitudes of the same loading case. Furthermore, it is assumed that the Optical Sciences Center can specify the dimensions and the support mechanism for the base plate. Of course, the base plate design will be compatible with the dewar plate already at Ames.

In this report the forces and/or moments transferred from the mount to the mirror due to cool down, gravity loading, tilt in the base plate, and flexure error as well as magnitude of stress in the flexures under various loadings are calculated analytically. By using the analytical results and utilizing the finite element techniques, the quality of the mirror figure under different conditions is established. By using the magnitude of stress in the flexures and the figure quality in the mirror as the basic criteria, a range of acceptable design dimensions for the mount is found and a specific design is designated. Furthermore, an estimate of the magnitude and distribution pattern of stresses in the mirror is also provided.

2. ANALYSIS

2.1. Force/Moment Transfer from Mount to Mirror

The proposed mount is shown in Fig. 1, and the flexures are shown in detail in Fig. 2.

2.1.1. Cool Down, Zero Gravity

The mirror has a zero coefficient of thermal expansion. Therefore, cool down in a 0-G environment will induce a radial displacement of the flexure base with respect to the mirror (Fig. 3). For all practical purposes, the flexure top and bottom plates can be assumed to be very stiff (i.e., $T = \infty$). This assumption is equivalent to analyzing the flexure system as a frame with very stiff girders that in turn degenerates to beam analysis. As shown in Table 2, the above assumption is a conservative one.

Table 2. Comparison between Frame and Beam Analysis

T (in.)	t (in.)	x (in.)	b (in.)	L (in.)	Δ (in.)	F_c (lb)
∞	0.05	2	2	2.5	0.02652	7.638
0.25	0.05	2	2	2.5	0.02652	7.623

The radial force transferred to the mirror from each flexure blade, F_c, can be calculated as

$$F_c = E \frac{bt^3}{\ell^3} \Delta \qquad (1)$$

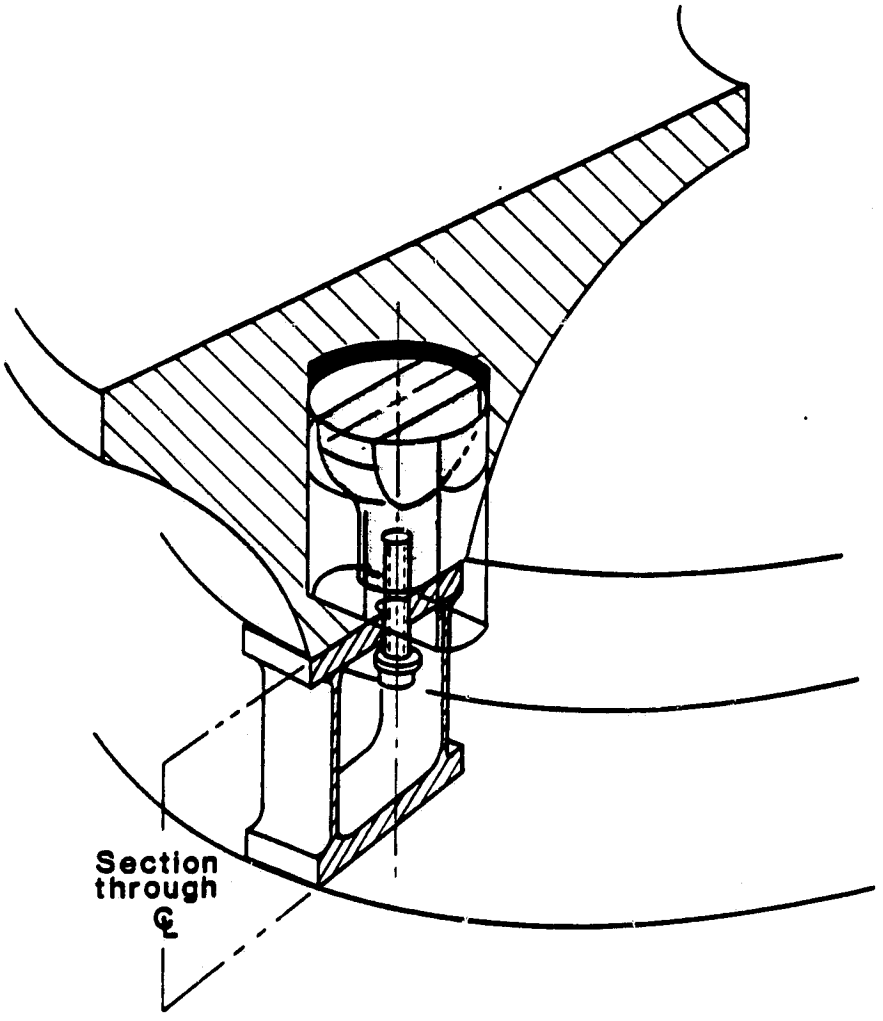

Figure 1. Isometric view of double arch mirror mount.

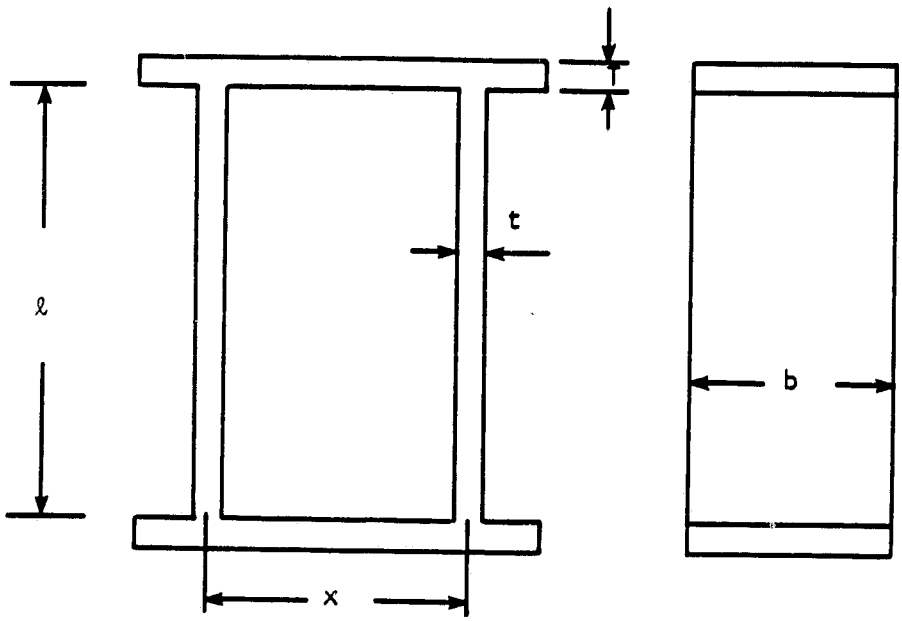

Figure 2. Flexure geometry.

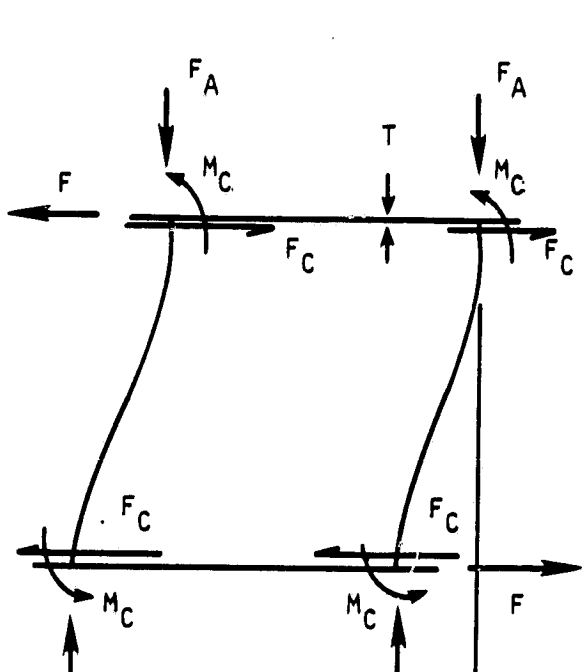

Figure 3. Flexure geometry at cool down.

where

E = modulus of elasticity

b = width of flexure

t = thickness of flexure blade

ℓ = flexure height

Δ = radial displacement due to cool down.

The total force transferred to the mirror from each flexure, F, is

$$F = 2F_c.$$

2.1.2. Cool Down, 1-G Loading

The mirror will be tested in cryogenic temperatures under a 1-G gravitational field. The gravity induces axial force to the flexures. In a face-up testing, when the flexures are in compression, the force transferred to the mirror, F_{cc}, is reduced to

$$F_{cc} = \frac{F_A}{\ell(\tan\lambda/\lambda - 1)} \Delta, \qquad (2)$$

where

F_A = axial force per flexure blade = GW/6

G = gravity loading

W = weight of mirror = 40 lb

$\lambda = \frac{n\ell}{2}$

$$n = (F_A/EI)^{1/2} = (12F_A/Ebt^3)^{1/2}.$$

In a face-down testing, where a tensile axial force is generated, the transferred force, F_{ct}, increases to

$$F_{ct} = \frac{F_A}{\ell(1 - \tanh\lambda/\lambda)} \Delta. \qquad (3)$$

2.1.3. Temperature Effects

Cryogenic temperatures might induce radial tilt (θ_r) and tangential tilt (θ_t) in the base plate. In calculating the effect of such tilts on the mirror, the flexure/base plate interaction plays an important role.

(a) Flexure/Base Plate Interaction

Tilt in an infinitely stiff base plate will be totally transferred to an infinitely flexible flexure. On the other hand, if a stiff flexure is mounted on a flexible base plate, no tilt will be transferred to the flexure. Furthermore, a tilt in a stiff base plate will induce negligible moment in a flexible flexure, and as the flexure becomes stiffer, the moment increases.

Both the flexures and base plate have finite stiffness. Therefore, a local tilt in the base plate will be partially transferred to the flexure and partially compensated for in the plate (Fig. 4). This effect can be written as

$$\theta = \theta_f + \theta_p$$

where

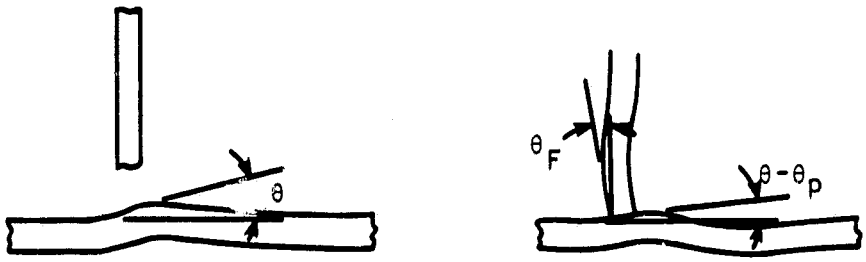

(a)

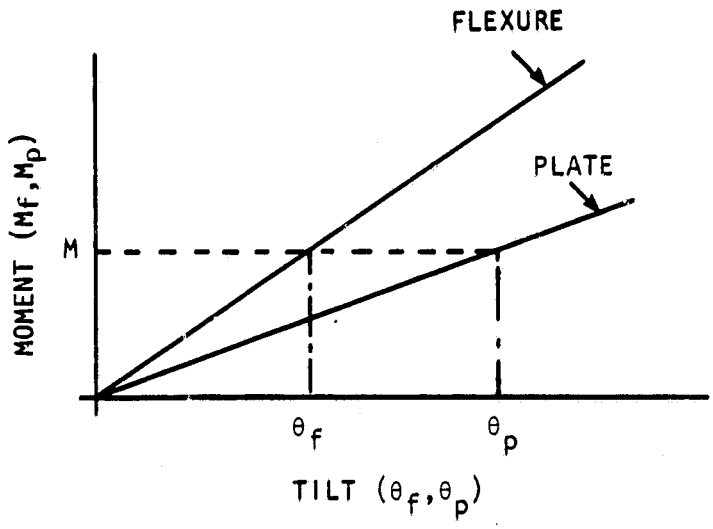

(b)

Figure 4. Flexure/base plate interaction

θ = local tilt in plate

θ_f = tilt in flexure

θ_p = tilt in plate.

The equilibrium condition requires that the moment in plate, M_p, be equal to that of flexure, M_f, at the plate-flexure interface

$$M_p = M_f = M.$$

All the stresses are limited to the elastic range of the materials. Therefore, tilt and moment in both flexure and plate can be related by linear functions (Fig. 4)

$$\theta_f = f_f M$$

$$\theta_p = f_p M$$

where

f_f = rotational flexibility of flexure

f_p = rotational flexibility of plate.

Therefore, it follows that

$$\theta = (f_f + f_p)M. \tag{4}$$

Any tilt angle calculated for an infinitely stiff plate should be reduced by a factor, R:

$$R = \frac{\theta_{f(\text{finite plate stiffness})}}{\theta_{f(\text{infinitely stiff plate})}} = \frac{f_f}{f_f + f_p}, \tag{5}$$

Equation (5) clearly shows the importance of increasing the flexibility of the base plate, f_p, which is a function of plate size, material, and support system. In this design, a 16-in. diameter, 1/4-in. thick aluminum (tooling) plate with three supports at 120° and on a 7-in. radius is used to maximize the flexibility of the plate. The flexures are mounted to the base plate with a 60° phase angle with respect to the plate supports. For the above

$$f_{pr} = 0.3947 \times 10^{-4} \text{ in.}^{-1}\text{lb}^{-1}$$
$$f_{pt} = 0.2058 \times 10^{-4} \text{ in.}^{-1}\text{lb}^{-1},$$

where f_{pr} and f_{pt} are the plate flexibility, f_p, in radial and tangential directions. Plate flexibility was calculated by finite element techniques.

(b) Radial Tilt

The moment, M_r, transferred to the mirror due to a radial tilt, θ_r, in the base plate is given by

$$M_r = E \frac{btx^2}{\ell} R_r \theta_r, \tag{6}$$

where

x = flexure blade separation

$$R_r = \frac{f_{fr}}{f_{fr} + f_{pr}} \tag{7}$$

$$f_{fr} = \frac{\ell}{2Ebtx^2} . \tag{8}$$

The transferred force, f_r, will be

$$F_r = \frac{3}{\ell} M_r. \tag{9}$$

(c) Tangential Tilt

The moment, M_t, transferred to the mirror due to a tangential tilt, θ_t, in the base plate is given by

$$M_t = \frac{E}{3} \frac{tb^3}{\ell} R_r \theta_t, \tag{10}$$

where

$$R_T = \frac{f_{ft}}{f_{ft} + f_{pt}} \tag{11}$$

$$f_{ft} = \frac{3\ell}{2Etb^3}. \tag{12}$$

The transferred force, f_t, will be

$$F_t = \frac{3}{\ell} M_t. \tag{13}$$

(d) Flexure Error

Nonparallelism of the flexures is a possible source of error that might result in transfer of some additional force to the mirror due to

cool down. For a given error, ε, the induced force, F_ε, is

$$F_\varepsilon = 3E \frac{btx}{\ell} \left(1 - \frac{\Delta^2}{\ell^2}\right)^{1/2} \left[1 - \left(1 - \frac{2\Delta\varepsilon}{(\ell^2-\Delta^2)}\right)\right]^{1/2} , \qquad (14)$$

where ε is the nonparallelism error.

2.2. Stress in Flexures

2.2.1. Stress in Cryogenic Temperatures

The critical stress develops when the flexures are loaded axially in a cryogenic environment. By using equilibrium conditions, the maximum moment in the flexures, M_{ct}, can be calculated by (Fig. 3)

$$M_{ct} = \frac{1}{2} (f_{ct}\ell + F_A\ell), \qquad (15)$$

where F_A and F_{ct} are defined by Eqs. (2) and (3).

Therefore, the maximum normal stress, σ_{ct}, and shear stress, τ_{ct}, are given by

$$\sigma_{ct} = \frac{6M_{ct}}{bt^2} + \frac{F_A}{bt} \qquad (16)$$

$$\tau_{ct} = 1.5 \frac{F_{ct}}{bt} . \qquad (17)$$

In the absence of axial loading (0-G, cool down) Eqs. (16) and (17) can be simplified to

$$\sigma_c = 3E \frac{t}{\ell^2} \Delta \tag{18}$$

$$\tau_c = 1.5 \frac{F_c}{bt}. \tag{19}$$

The maximum normal stress occurs at the inner corner of the flexure blades above the base plate whereas the maximum shearing stress is at the physical center of the cross section through the blade. Stress concentration factors will be included in the final calculation.

2.2.2. Side Loading

During launch, emergency landing, or on edge testing, the mirror will be subjected to loading perpendicular to its optical axis. In the worst case, when the side loading is applied in the compliance direction of one of the flexures, the force, F_s, taken by each blade of the other two flexures can be calculated by

$$F_s = \frac{GW}{2\sqrt{3}}. \tag{20}$$

The maximum normal stress, σ_s, and shearing stress, τ_s, are given by

$$\sigma_s = 3F_s \frac{\ell}{tb^2} \tag{21}$$

$$\tau_s = 1.5 \frac{F_s}{bt}. \tag{22}$$

2.2.3. Stress due to Mount Error

The existence of local tilt in the base plate will induce stress in the flexures

$$\sigma_r = E \frac{x}{\ell} R_r \theta_r \tag{23}$$

$$\sigma_t = E \frac{b}{\ell} R_t \theta_t \tag{24}$$

$$\tau_r = 0.75 \frac{F_r}{bt} \tag{25}$$

$$\tau_t = 0.75 \frac{F_t}{bt}, \tag{26}$$

where

σ_r = maximum normal stress due to radial tilt

σ_t = maximum normal stress due to tangential tilt

τ_r = maximum shear stress due to radial tilt

τ_t = maximum shear stress due to tangential tilt.

Nonparallelism error in the flexures causes additional stress

$$\sigma_\varepsilon = 3 \frac{F_e \ell}{bt^2} \tag{27}$$

$$\tau_\varepsilon = 1.5 \frac{F_\varepsilon}{bt^2}, \tag{28}$$

where σ_ε and τ_ε are the maximum normal and shearing stress due to flexure error.

2.2.4. Critical Normal Stress

In the worst case, where the stress components are all additive, the maximum normal stress is given by

$$\sigma_{max} = K(\sigma_c + \sigma_s + \sigma_r + \sigma_t + \sigma_f), \tag{29}$$

where K is the stress concentration factor. As a conservative estimate K will be assumed to be 1.5.

The maximum shearing stress, τ, can be calculated by (Fig. 5)

$$\tau_{max} = (\tau_1^2 + \tau_2^2)^{1/2} \tag{30}$$

where

$$\tau_1 = \tau_t + \tau_s$$

$$\tau_2 = \tau_{ct} + \tau_r + \tau_\varepsilon.$$

2.3. Influence of Mount on Figure Quality

The principles of linearity and superposition are used in conjunction with finite element techniques to analyze the effect of mount-induced forces/moments on the mirror.

The finite element model for the double arch mirror consisted of 210 nodes and 168 quadrilateral plate and shell elements (Fig. 6). The

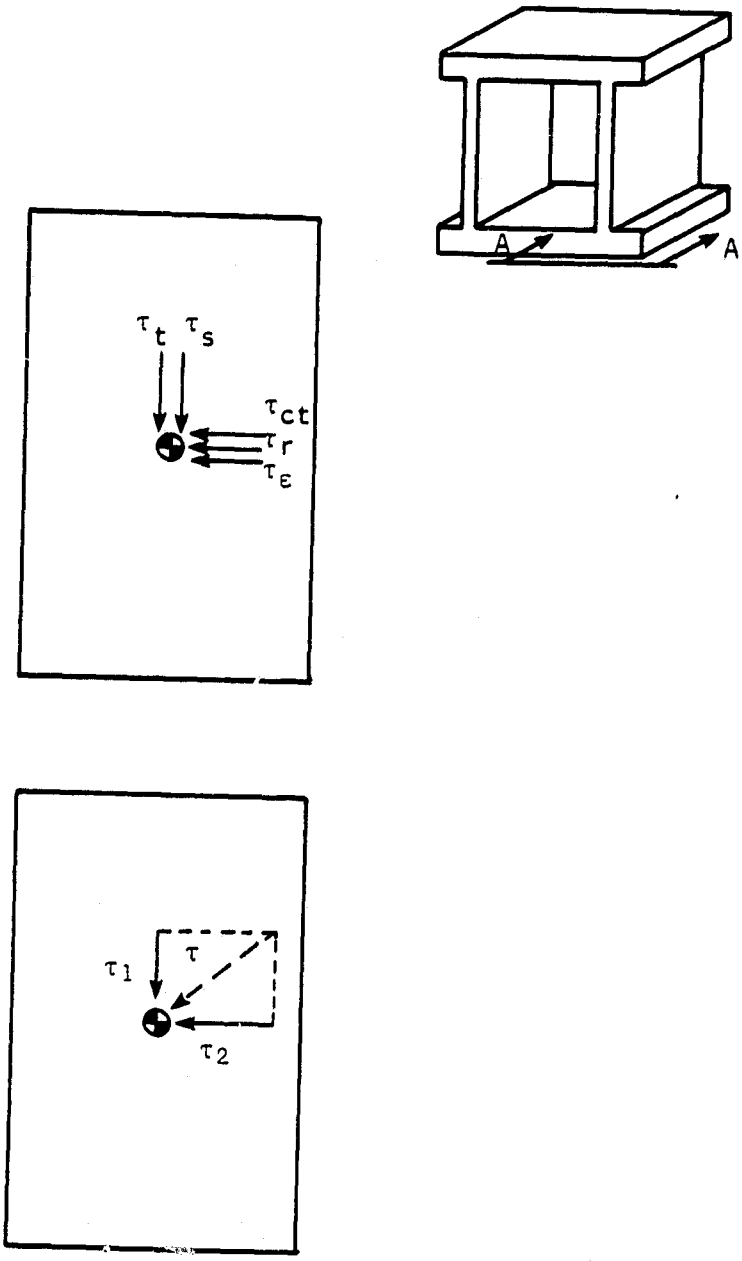

Figure 5. Shearing stress in flexures.

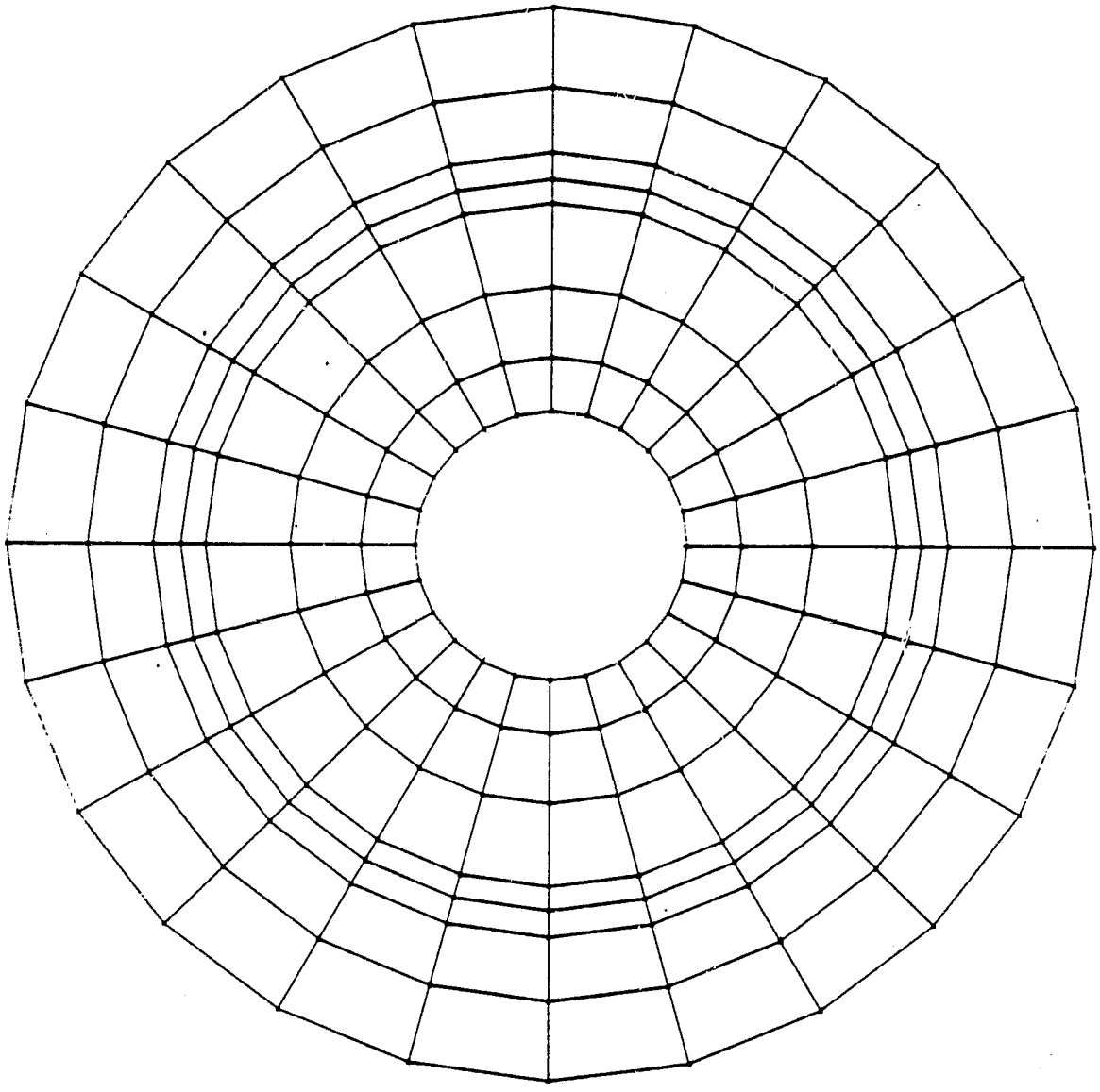

Figure 6. Finite element model of double arch mirror.

software used was SAP IV. This model was used throughout this study to determine the changes in the optical surface due to mount effects. Note that the flexures were implicitly included in the model by directly applying the flexure-induced forces/moments to the mirror base.

Various loadings that the mirror can encounter, either in testing or operation, can be resolved into three different categories (cases 1 through 3). Once the sensitivity of the mirror figure to each loading case is established, then the optical performance of the mirror for any specific flexure design can be determined.

2.3.1. Case 1

A set of forces/moments of equal magnitude are applied to the mirror base in the radial direction and 120° apart (Fig. 7a). This case represents the effect of cool down. To arrive at the most fundamental case, we will substitute F and M with F_o and M_o

$$F_o = F$$

$$M_o = M + Fd$$

where d is the distance between the mirror base and the center of gravity. Note that the line of action of force f_o passes through the center of gravity of the mirror. Obviously, analyzing the mirror performance with respect to M_o and F_o will correspond to a more basic case than M and F.

Figure 8 shows the contour map of the mirror surface when M_o = 1 in.-lb. Also shown in Fig. 8 are the Zernike coefficients and the RMS

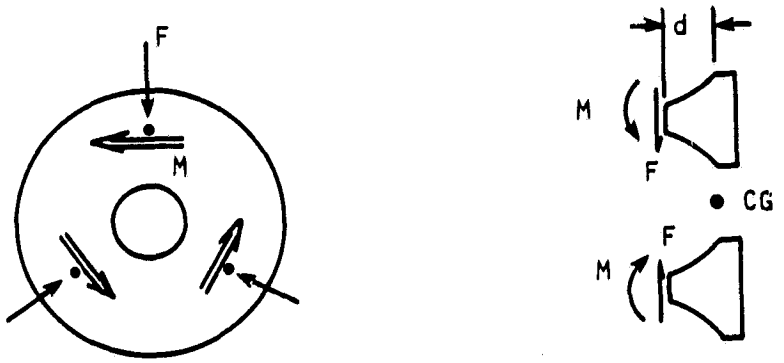

(a)

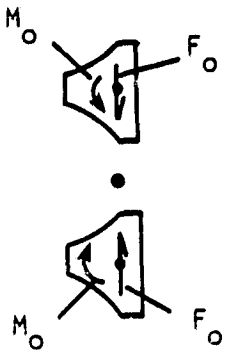

(b)

Figure 7. Resolution of forces/moments.

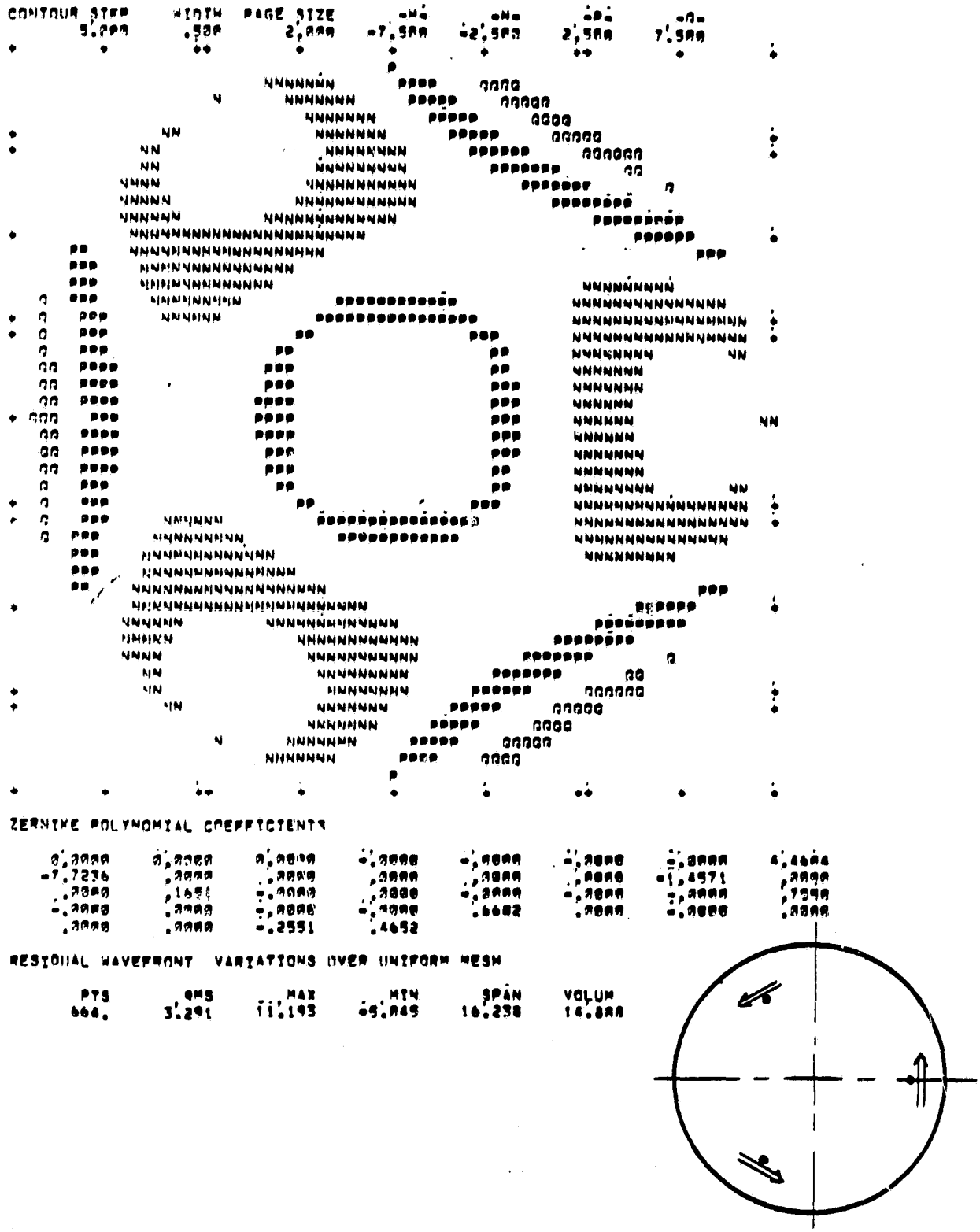

Figure 8. Sensitivity factors for cool down (units of inch x 10^8).

A schematic of the forces/moments is shown at the lower right of each contour map. The right-hand rule is used to represent moments.

(RMS_{c0}) value. The values given in Fig. 8 can also serve as the sensitivity factors for the mirror, i.e., each value has units of (in. x 10^{-8})/(in.-lb). Therefore, for a given moment of $M = M_m$ ($M_o = M_m$ and $F = F_o = 0$) the RMS as well as the Zernike coefficients, R_n^m, can be calculated by

$$RMS = M_m \times RMS_{co}$$

$$R_n^m = M_m \times (R_n^m)_{co}$$

where

RMS_{co} = RMS value when a unit moment is applied.

$(R_n^m)_{co}$ is the Zernike coefficient of mth angular and nth tangential order when a unit moment is applied. For the explicit form of Zernike coefficients see Table 3.

Based on past experience with double arch mirrors, any force that goes through the center of gravity of the mirror (i.e., its line of action is on the plane parallel to the mirror base and passes through the center of gravity) will have a small effect on the overall surface quality. Figures 9 and 10 can be used to illustrate the above. In both figures, a unit radial load is acting on the base. However, Fig. 9 includes the radial force through the center of gravity (i.e., $F = 1$, $M = 0$, $F_o = 1$, $M_o = 1 \times d = 1 \times 1.7513 = 1.7513$) where as in Fig. 10 only the moment is considered (i.e., $M_o = 1.7513$, $F_o = 0$). As it is shown, the RMS values differ only by a small factor ($\Delta(RMS)/RMS < 0.01$). In all the subsequent analyses the effect of any force through the center of gravity has been assumed to be negligible (i.e., $F_o = 0$).

Table 3. Zernike Polynomials Used by Fringe in the Order Stored in the Computer

	Polynomial
R_1^1	$r\cos\theta$
R_1^{-1}	$r\sin\theta$
R_2^0	$2r^2 - 1$
R_2^2	$r^2\cos 2\theta$
R_2^{-2}	$r^2\sin 2\theta$
R_3^1	$(3r^2 - 2)r\cos\theta$
R_3^{-1}	$(3r^2 - 2)r\sin\theta$
R_4^0	$6r^4 - 6r^2 + 1$
R_3^3	$r^3\cos 3\theta$
R^{3-3}	$r^3\sin 3\theta$
R_4^2	$(4r^2 - 3)r^2\cos 2\theta$
R_4^{-2}	$(4r^2 - 3)r^2\sin 2\theta$
R_5^1	$(10r^4 - 12r^2 + 3)r\cos\theta$
R_5^{-1}	$(10r^4 - 12r^2 + 3)r\sin\theta$
R_6^0	$20r^6 - 30r^4 + 12r^2 - 1$
R_4^4	$r^4\cos 4\theta$
R_4^{-4}	$r^4\sin 4\theta$
R_5^3	$(5r^2 - 4)r^3\cos 3\theta$
R_5^{-3}	$(5r^2 - 4)r^3\sin 3\theta$
R_6^2	$(15r^4 - 20r^2 + 6)r^2\cos 2\theta$
R_6^{-2}	$(15r^4 - 20r^2 + 6)r^2\sin 2\theta$
R_7^{-1}	$(35r^6 - 60r^4 + 30r^2 - 4)r\cos\theta$
R_7^{-1}	$(35r^6 - 60r^4 + 30r^2 - 4)r\sin\theta$
R_8^0	$70r^8 - 140r^6 + 90r^4 - 20r^2 + 1$
R_5^5	$r^5\cos 5\theta$
R_5^{-5}	$r^5\sin 5\theta$
R_6^4	$(6r^2 - 5)r^4\cos 4\theta$
R_6^{-4}	$(6r^2 - 5)r^4\sin 4\theta$
R_7^3	$(21r^4 - 30r^2 + 10)r^3\cos 3\theta$
R_7^{-3}	$(21r^4 - 30r^2 + 10)r^3\sin 3\theta$
R_8^2	$(56r^6 - 105r^4 + 60r^2 - 10)r^2\cos 2\theta$
R_8^{-2}	$(56r^6 - 105r^4 + 60r^2 - 10)r^2\sin 2\theta$
R_9^1	$(126r^8 - 280r^6 + 210r^4 - 60r^2 + 5)r\cos\theta$
R_9^{-1}	$(126r^8 - 280r^6 + 210r^4 - 60r^2 + 5)r\sin\theta$
R_{10}^0	$252\ r^{10} - 630r^8 + 560r^6 - 210r^4 + 30r^2 - 1$
R_{12}^0	$924\ r^{12} - 2772r^{10} + 3150r^8 - 1680r^6 + 420r^4 - 42r^2 + 1$

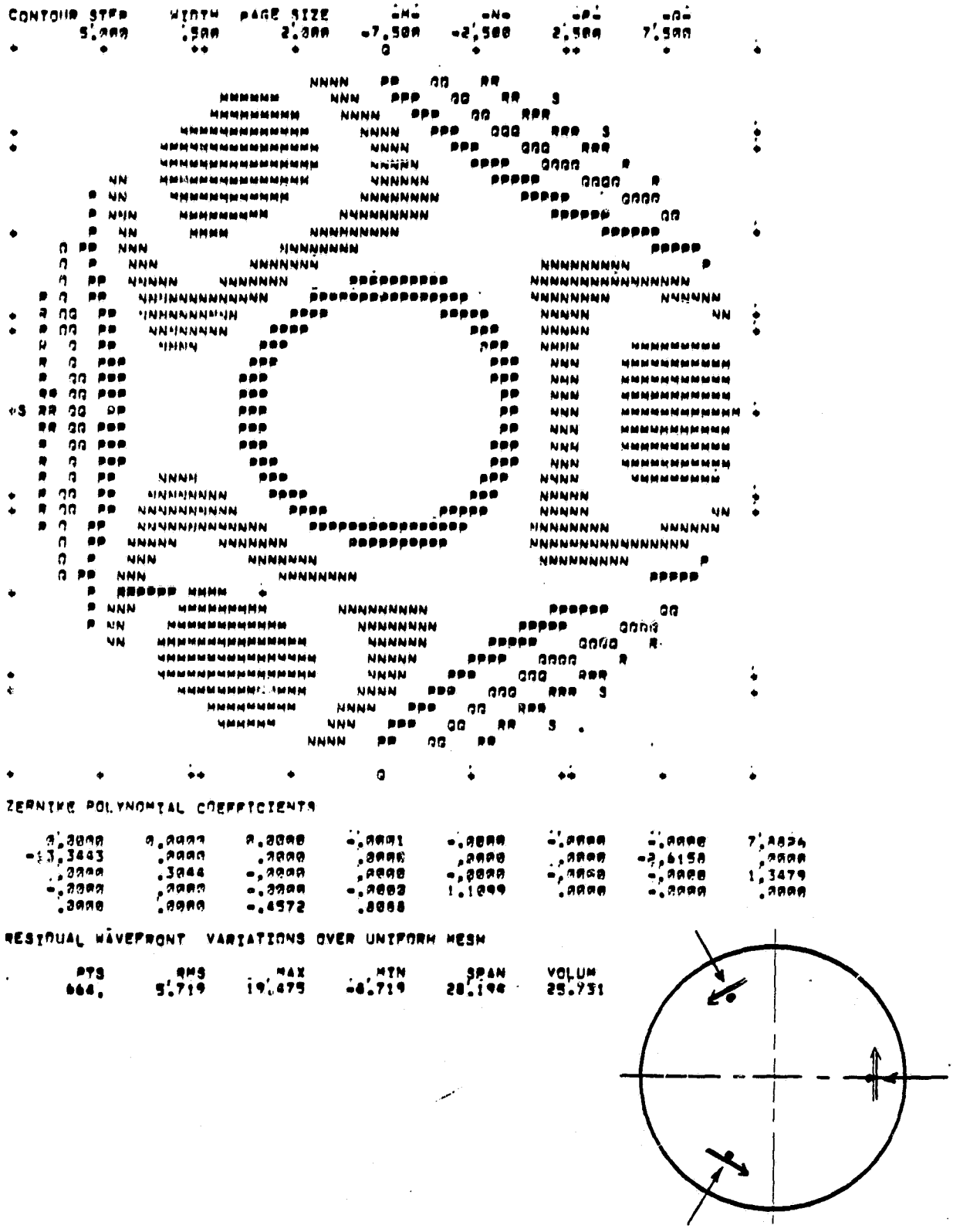

Figure 9. Application of a unit force at the mirror base (units of inch x 10^8).

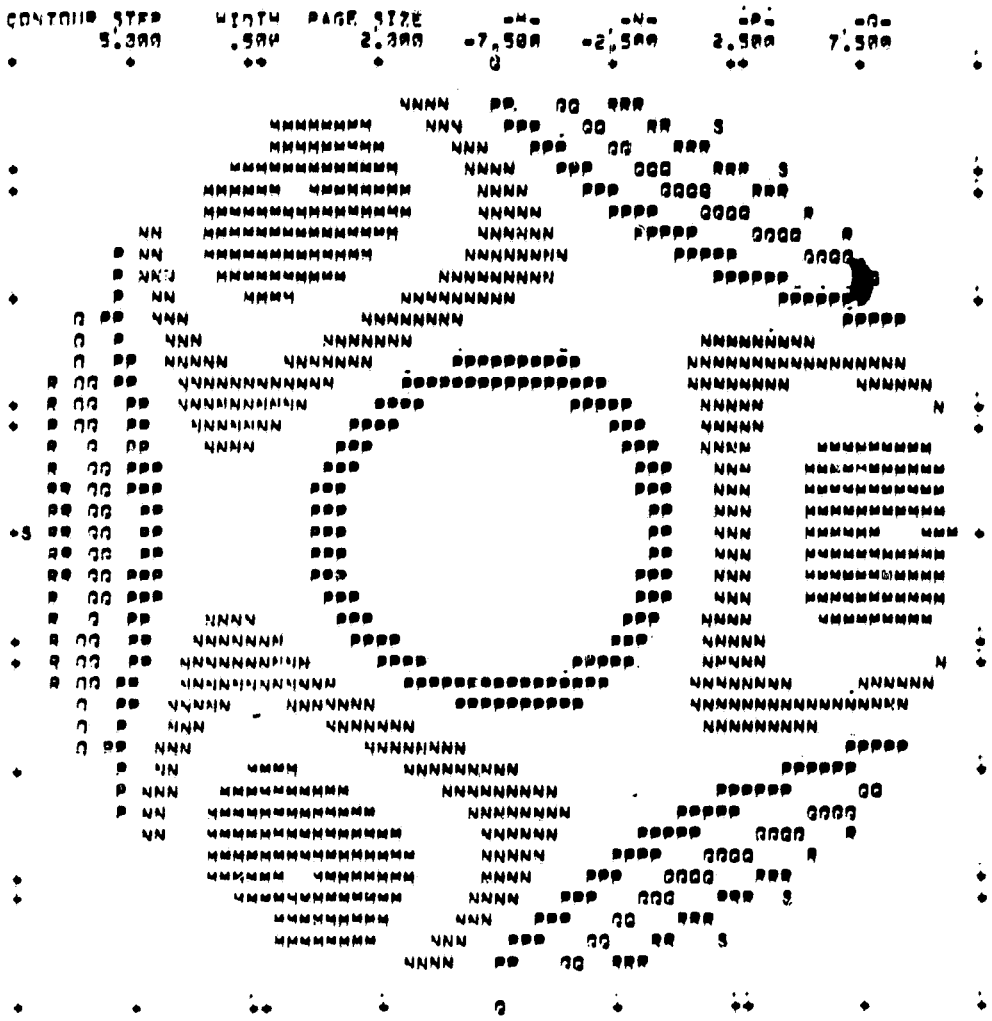

ZERNIKE POLYNOMIAL COEFFICIENTS

0.0000	0.0000	0.0000	-.0001	-.0000	-.0000	-.0000	7.8115
-13.5244	.0000	.0000	.0000	.0000	.0000	-2.5518	.0000
.0000	.2491	-.0000	.0000	-.0000	-.0000	-.0000	1.3223
-.0000	.0000	-.0000	-.0000	1.1563	.0000	-.0000	.0000
.0000	.0000	-.4468	.8148				

RESIDUAL WAVEFRONT VARIATIONS OVER UNIFORM MESH

PTS	RMS	MAX	MIN	SPAN	VOLUM
664.	5.744	19.682	-8.835	28.437	26.973

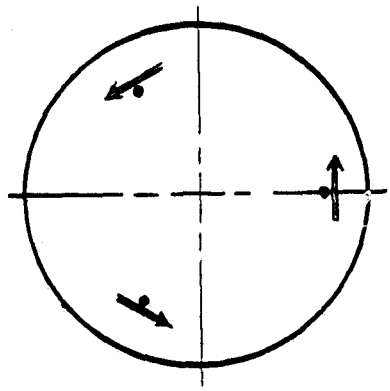

Figure 10. Application of a unit force to the mirror base. The force through the center of gravity is ignored (units of inch x 10^8).

2.3.2. Case II

Application of a radial force/moment at only one radial location. This case corresponds to the unpredictable mount error in the radial direction. The contour map, Zernike coefficients, and RMS (RMS_{ro}) value are shown in Fig. 11.

2.3.3. Case III

Application of a tangential force/moment at only one radial location. This case corresponds to the unpredictable mount error in the radial direction. The contour map, Zernike coefficients, and the RMS (RMS_{to}) value are shown in Fig. 12.

By using the three loading cases and the equations given in section 2.3.1, the following equations can be written:

$$RMS_c = (dF)(RMS_{co}) \text{ for cool-down effect} \quad (31)$$

$$RMS_r = (M_r + dF_r)(RMS_{ro}) \text{ for radial tilt} \quad (32)$$

$$RMS_t = (M_t + dF_t)(RMS_{to}) \text{ for tangential tilt} \quad (33)$$

$$RMS_f = (2dF_f)(RMS_{ro}) \text{ for flexure error.} \quad (34)$$

Table 4 gives a listing of the RMS sensitivity factors.

Table 4. RMS Sensitivity Factors

	RMS ($in.\times 10^6$)
RMS_{co}	0.0329
RMS_{ro}	0.0271
RMS_{to}	0.0927

ZERNIKE POLYNOMIAL COEFFICIENTS

0.0000	0.0000	0.0000	-4.2086	-.0000	-4.7895	-.0000	1.4098
-2.5984	-.0000	-.7593	.0000	2.1382	-.0000	-.4833	-.6317
.0000	.0398	.0000	.7798	-.0000	-1.0940	.0000	.3148
-.3414	-.0000	-.3097	-.0000	.2240	-.0000	-.4209	.0000
.0934	.0000	-.0700	.1429				

RESIDUAL WAVEFRONT VARIATIONS OVER UNIFORM MESH

PTS	RMS	MAX	MIN	SPAN	VOLUM
664.	2.789	9.885	-9.281	19.086	27.389

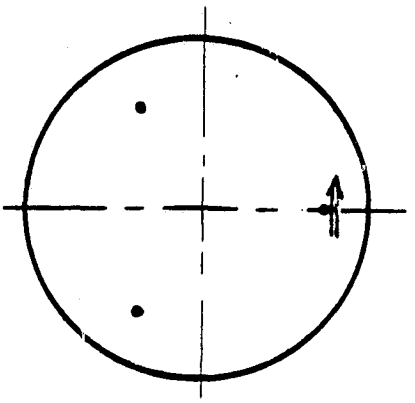

Figure 11. Sensitivity factors for radial tilt (units of inch x 10^{8}).

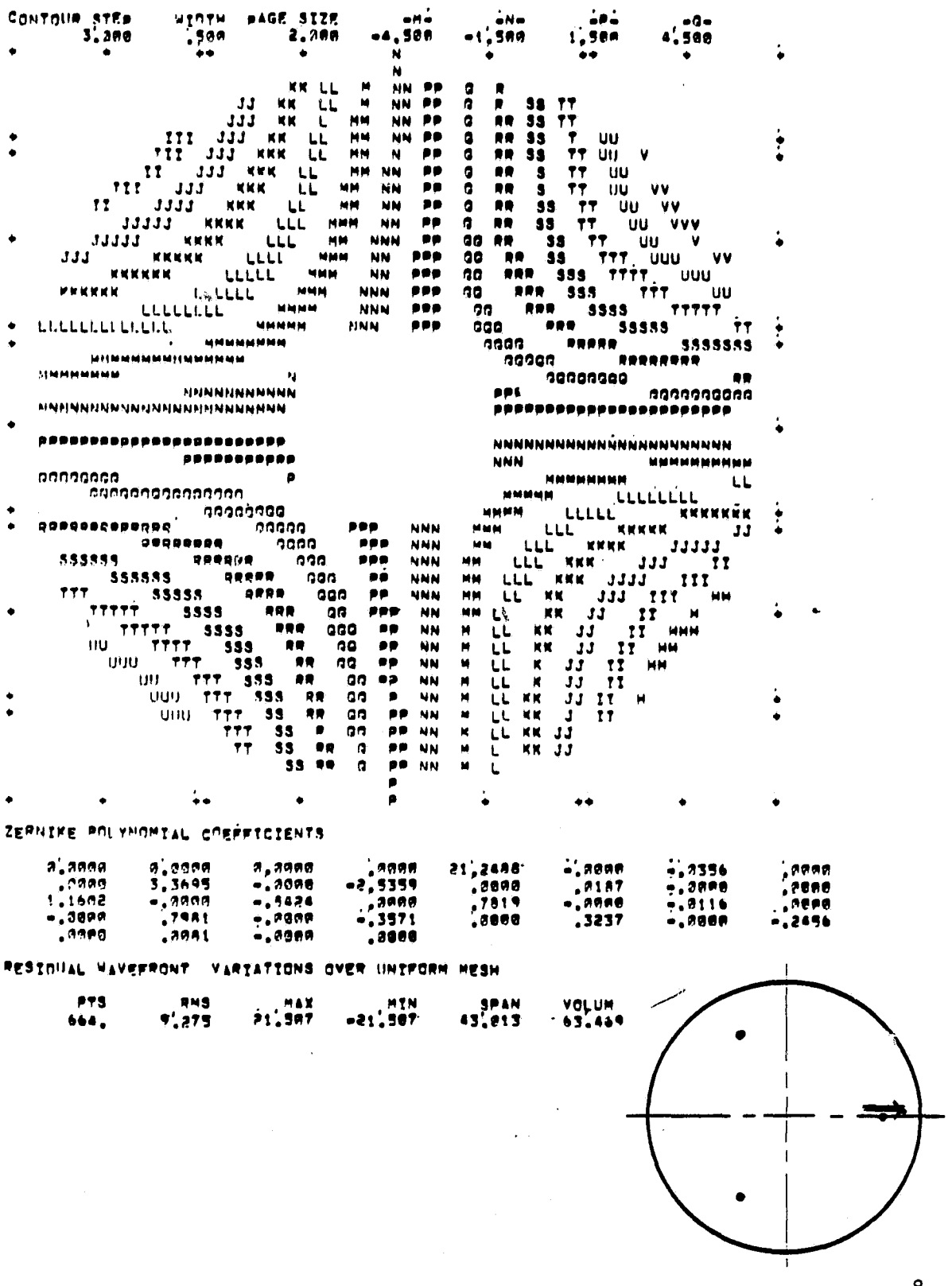

Figure 12. Sensitivity factor for tangential tilt (units of inch x 10^8).

3. FLEXURE DESIGN

3.1. Design Range

The flexure design was directly controlled by several factors.

3.1.1. Manufacturing Requirements

Based on the dimensional limitations imposed on the design by the manufacturing process and also based on past experience with flexures, the design parameters were constrained to a feasible region given by

$$\begin{aligned} &0.03 \text{ in.} \leq t \leq 0.04 \text{ in.} \\ &2.0 \text{ in.} \leq \ell \leq 4.0 \text{ in.} \\ &0.6 \text{ in.} \leq x \leq 2.0 \text{ in.} \\ &0.4 \text{ in.} \leq b \leq 2.0 \text{ in.} \end{aligned} \tag{35}$$

3.1.2. Surface Quality Requirements

Establishing accurate estimates of possible mount error or temperature effects, if possible, will require considerable time and effort. Therefore, instead of imposing performance requirements on the overall surface quality, we will limit the contribution of independent sources of figure deterioration. Furthermore, we will quantify the surface quality by the root mean square (RMS) value of the differences between the deformed mirror surface and the undeformed surface measured at 644 regularly spaced grid points. In doing so, it is assumed that tilt and focus terms can be corrected by the telescope system. The following requirements were imposed on the design:

$RMS_c \leq 1 \times 10^{-6}$ in. due to cool down

$RMS_s \leq 2.5 \times 10^{-6}$ in. due to radial tilt

$$RMS_t \leq 2.5 \times 10^{-6} \text{ in. due to tangential tilt} \qquad (36)$$

$$RMS_f \leq 2.5 \times 10^{-6} \text{ in. due to flexure error.}$$

3.1.3. Stress Requirements

The maximum stress in the flexures will be designed not to exceed the microyield limit, either in operation or during launch. However, in an emergency, landing stresses as high as the yield point will be allowable. A safety factor of 2 will be used:

$$\sigma_c \leq 57{,}500 \text{ psi during 0-G cool down}$$

$$\sigma_{ct} \leq 57{,}500 \text{ psi during launch}$$

$$\sigma_{ct} \leq 120{,}000 \text{ psi during emergency landing} \qquad (37)$$

$$\tau \leq 42{,}000 \text{ psi during emergency landing.}$$

It would have been ideal to optimize the design for minimum RMS in the mirror and minimum stress in the flexures. However, these two objectives are in direct conflict. An unsuccessful attempt was made to optimize the design for a minimum RMS in the mirror by using the OPTLIB (Ref. 1) optimization package. The failure of this approach might be due to the highly nonlinear nature of the problem. Therefore, in the absence of a better approach, a parametric study of the feasible region defined by Eqs. (35), (36), and (37) was performed. As a result of this study the following design parameters were chosen:

$$t = 0.04 \text{ in.}$$

$$\ell = 3.60 \text{ in.}$$

$$x = 1.00 \text{ in.} \qquad (38)$$

$$b = 0.60 \text{ in.}$$

An inclusive list of the feasible design region is given in Appendix A.

3.2 Design Calculations

In this section we illustrate the application of the analytical approach, as outlined in section 2, by applying it to the proposed design as given by Eq. (38). Numbers on the right-hand side denote the equation used.

3.2.1. 0-G Cool Down

$$\Delta = 0.0286 \text{ in.}$$

$$F_c = 18 \times 10^6 \times \frac{(0.6)(0.04)^3}{(3.6)^3} \times 0.0286$$

$$= 0.424 \text{ lb} \qquad (1)$$

$$\sigma_c = 3 \times 18 \times 10^6 \times \frac{0.04}{(3.6)^2} \times 0.0286 = 4766.7 \text{ psi} \qquad (18)$$

$$\tau_c = 1.5 \times \frac{0.424}{(0.6)(0.04)} = 26.5 \text{ psi} \qquad (19)$$

$$RMS_c = (1.7513 \times 2 \times 0.424)(0.0329 \times 10^{-6})$$

$$= 0.049 \times 10^{-6} \text{ in.} \qquad (31)$$

For a contour map see Fig. 13.

3.2.2. 1-G Cool Down. Face Down Testing

$$F_A = \frac{1 \times 40}{6} = 6.667 \text{ lb} \qquad (2)$$

$$n = \left[\frac{12 \times 6.667}{18 \times 10^6 \times 0.6 \times (0.04)^3}\right]^{1/2} = 0.340 \qquad (2)$$

$$\lambda = \frac{0.340 \times 3.6}{2} = 0.612 \qquad (2)$$

$$F_{ct} = \frac{6.667}{3.6(1 - 1/0.612 \tanh 0.612)} \times 0.0286 = 0.487 \text{ lb} \qquad (3)$$

$$M_{ct} = \frac{1}{2}(0.487 \times 3.6 + 6.667 \times 0.0286) = 0.972 \text{ in.-lb} \qquad (15)$$

$$\sigma_{ct} = \frac{6 \times 0.972}{0.6 \times (0.04)^2} + \frac{6.667}{0.6 \times 0.04} = 6354.0 \text{ psi} \qquad (16)$$

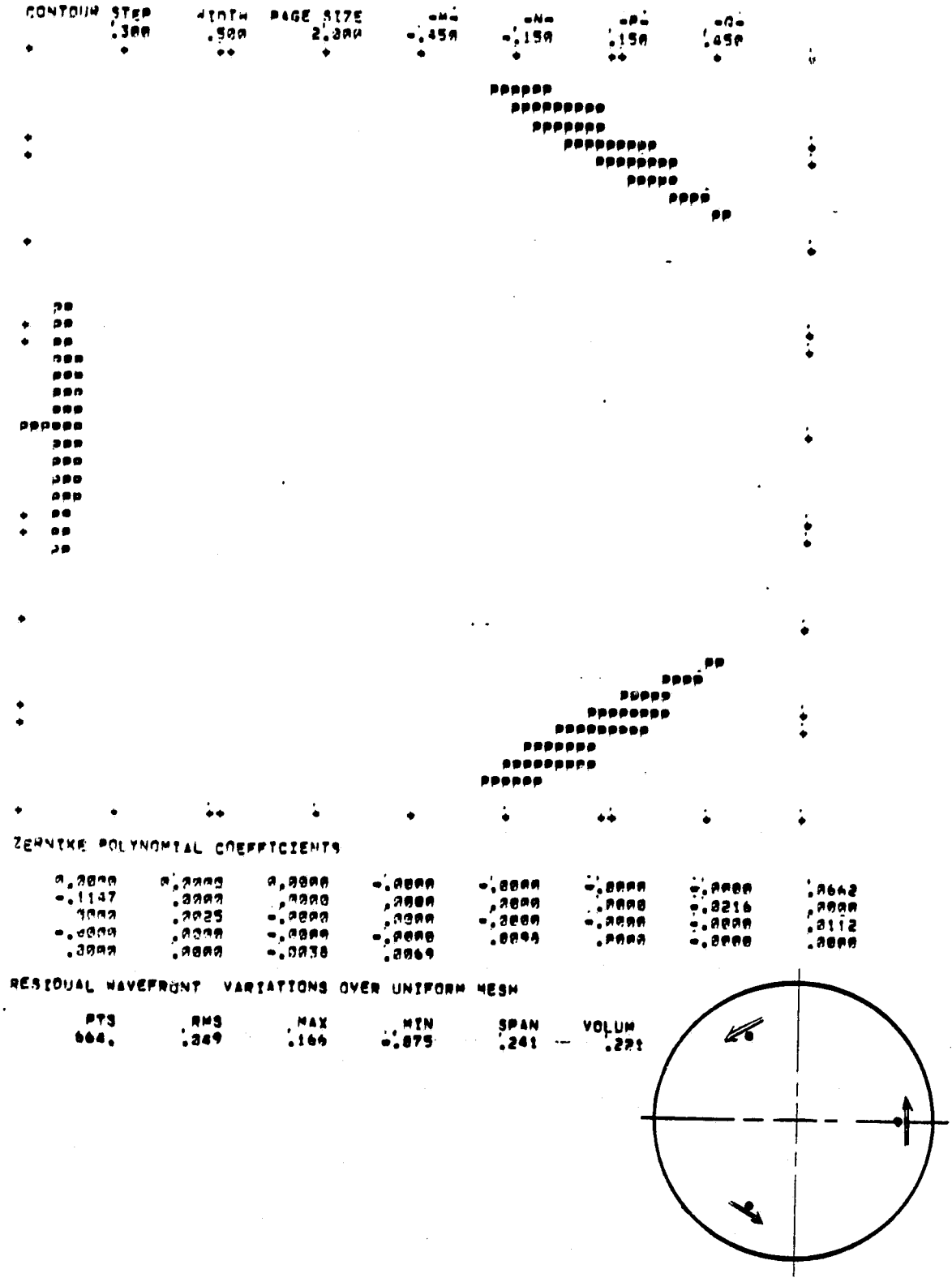

Figure 13. Contour map of double arch mirror surface at cool down with 0-G loading (units of inch x 10^6).

$$\tau_{ct} = 1.5 \times \frac{0.487}{0.6 \times 0.04} = 30.4 \text{ psi} \quad (17)$$

$$RMS_{ct} = (1.7513 \times 2 \times 0.487)(0.0329 \times 10^{-6})$$

$$= 0.056 \times 10^{-6} \quad (31)$$

For a contour map see Fig. 14.

3.2.3. Launch. Flexures in Tension

$$F_A = \frac{3.2 \times 40}{6} = 21.333 \text{ lb} \quad (2)$$

$$\sigma_{ct} = 9837.8 \text{ psi} \quad (16)$$

$$\tau_{ct} = 39.1 \text{ psi} \quad (17)$$

$$F_s = \frac{0.8 \times 40}{2\sqrt{3}} = 9.238 \text{ lb} \quad (20)$$

$$\sigma_s = \frac{3 \times 9.238 \times 3.6}{(0.04)(0.6)^2} = 6928.2 \text{ psi} \quad 21)$$

$$\tau_s = 1.5 \times \frac{9.238}{0.6 \times 0.04} = 577.3 \text{ psi} \quad (22)$$

3.2.4. Emergency Landing. Flexures in Tension

$$F_A = \frac{4.5 \times 40}{6} = 30.0 \text{ lb} \quad (2)$$

$$\sigma_{ct} = 11891.3 \text{ psi} \quad (16)$$

$$\tau_{ct} = 44.2 \text{ psi} \quad (17)$$

$$F_s = \frac{4.5 \times 40}{2\sqrt{3}} = 51.962 \text{ lb} \quad (20)$$

$$\sigma_s = 38971.1 \text{ psi} \quad (21)$$

$$\tau_s = 3247.6 \text{ psi} \quad (22)$$

3.2.5. Radial Tilt

Assume $\theta_r = 0.001$ rad

$$f_{fr} = \frac{3.6}{2 \times 18 \times 10^6 \times 0.6 \times 0.04 \times (1)^2} = 4.167 \times 10^{-6} \text{ in.}^{-1}\text{lb}^{-1} \quad (8)$$

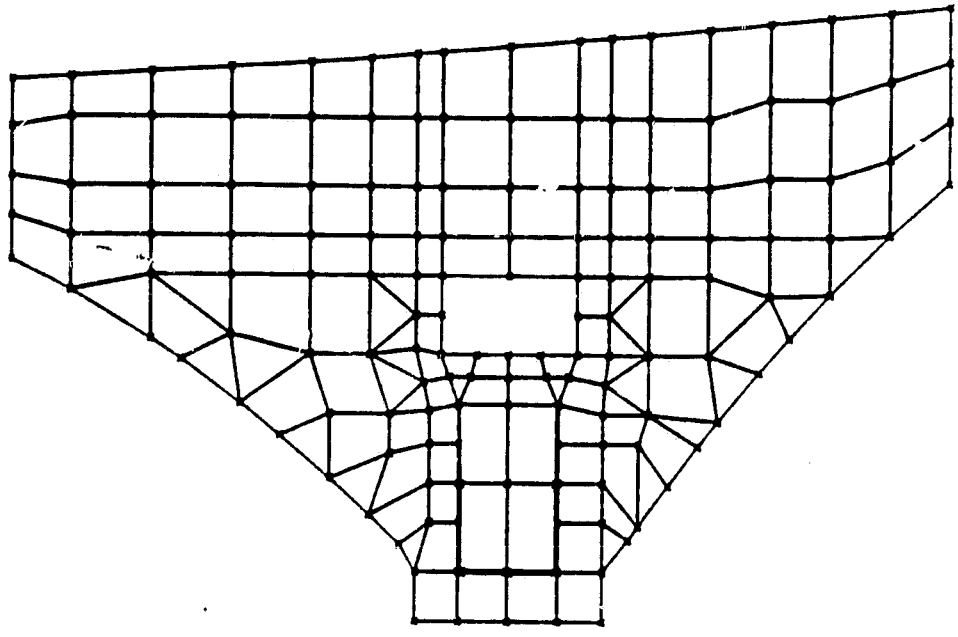

Figure 14. Axisymmetric finite element model of double arch mirror.

$$R_r = \frac{4.167 \times 10^{-6}}{4.167 \times 10^{-6} + 0.3947 \times 10^{-4}} = 0.095 \quad (7)$$

$$M_r = 18 \times 10^6 \times \frac{0.6 \times 0.04 \times (1)^2}{3.6} \times 0.095 \times 0.001 = 11.458 \text{ in.-lb} \quad (6)$$

$$F_r = \frac{3}{3.6} \times 11.458 = 9.549 \text{ lb} \quad (9)$$

$$\sigma_r = 18 \times 10^6 \times \frac{1}{3.6} \times 0.095 \times 0.001 = 477.7 \text{ psi} \quad (23)$$

$$\tau_r = 298.4 \text{ psi} \quad (25)$$

$$RMS_r = (11.458 + 1.7513 \times 9.549)(0.0271 \times 10^{-6})$$

$$= 0.763 \times 10^{-6} \text{ in.} \quad (32)$$

3.2.6. Tangential Tilt

Assume $\theta_t = 0.001$ rad

$$f_{ft} = \frac{3 \times 3.6}{2 \times 18 \times 10^6 \times 0.04 \times (0.6)^3} = 3.472 \times 10^{-5} \text{ in.}^{-1}\text{lb}^{-1} \quad (12)$$

$$R_t = \frac{3.472 \times 10^{-5}}{3.472 \times 10^{-5} + 0.2058 \times 10^{-4}} = 0.628 \quad (11)$$

$$M_t = \frac{18 \times 10^6}{3} \times \frac{0.04 \times (0.6)^3}{3.6} \times 0.628 \times 0.001 = 9.041 \text{ in.-lb} \quad (10)$$

$$F_t = \frac{3}{3.6} \times 9.041 = 7.534 \text{ lb} \quad (13)$$

$$\sigma_t = 18 \times 10^6 \times \frac{0.6}{3.6} \times 0.628 \times 0.001 = 1883.6 \text{ psi} \quad (24)$$

$$\tau_t = 0.75 \times \frac{7.534}{0.6 \times 0.04}) = 235.5 \text{ psi} \quad (26)$$

$$RMS_t = (9.041 + 1.7513 \times 7.534)(0.09275 \times 10^{-6})$$

$$= 2.062 \times 10^{-6} \text{ in.} \quad (33)$$

3.2.7. Flexure Error

Assume $\varepsilon = 0.001$ in.

$$F_\varepsilon = 3 \times 18 \times 10^6 \times \frac{0.6 \times 0.64 \times 1}{3.6}$$

$$\times \left(1 - \frac{(0.0286)^2}{(3.6)^2}\right)^{1/2} \left[1 - \left(1 - \frac{2 \times 0.0286 \times 0.001}{(3.6)^2 - (0.0286)^2}\right)^{1/2}\right]$$

$$= 0.794 \text{ lb} \tag{14}$$

$$\sigma_\varepsilon = 3 \times \frac{0.794 \times 3.6}{0.6 \times (0.04)^2} = 8938.1 \text{ psi} \tag{27}$$

$$\tau_\varepsilon = 1.5 \times \frac{0.794}{0.6 \times (0.04)^2} = 1241.4 \text{ psi} \tag{28}$$

$$RMS_f = (1.7513 \times 2 \times 0.794)(0.0271 \times 10^{-6})$$

$$= 0.075 \times 10^{-6} \text{ in.} \tag{34}$$

3.2.8. Presence of Mount Error

By including the stress concentration factor and the above calculation, the critical stresses can be obtained.

(a) 0-G cool down in the presence of mount error:

$$\sigma_{max} = 1.5(4766.7 + 0 + 477.4 + 1883.6 + 8938.1)$$

$$= 24097 \text{ psi} \tag{29}$$

$$\tau_1 = 235.5 + 0 = 235.5 \text{ psi} \tag{30}$$

$$\tau_2 = 26.5 + 298.4 + 1241.4 = 1566.3 \text{ psi}$$

$$\tau_{max} = (235.5^2 + 1655.3^2)^{1/2} = 1583.9 \text{ psi}$$

(b) Launch in the presence of mount error:

$$\sigma_{max} = 1.5(9837.8 + 6928.2 + 477.4 + 1883.6 + 8938.1)$$

$$= 42098.1 \text{ psi}$$

$$\tau_1 = 235.5 + 577.3 = 812.8 \text{ psi}$$

$$\tau_2 = 39.1 + 298.4 + 1241.4 = 1578.9 \text{ psi}$$

$$\tau_{max} = (812.8^2 + 1578.9^2)^{1/2} = 1775.8 \text{ psi}$$

(c) Emergency landing in the presence of mount error:

$$\sigma_{max} = 1.5(11891.3 + 38971.3 + 477.4 + 1883.6 + 8938.1)$$

$$= 93242.5 \text{ psi}$$

$$\tau_1 = 235.5 + 3247.6 = 3483.1 \text{ psi}$$

$$\tau_2 = 44.2 + 298.4 + 1241.4 = 1584.0 \text{ psi}$$

$$\tau_{max} = (3483.1^2 + 1584.0^2)^{1/2} = 3826.4 \text{ psi.}$$

Note that the RMS values are not directly additive. Appendix B gives examples of various cases where one or more mount errors are present.

4. STRESS IN THE MIRROR

To estimate the stress distribution inside the mirror due to the clamping force, a study was performed using the finite element method. The finite element model consisted of 136 triangular and quadrilateral axisymmetric elements (Fig. 14). It was assumed that the friction between the mirror base and the flexure top prevents any motion of the two with respect to each other. The stress profiles are shown in Figs. 15 through 20. The stress components are defined in Fig. 21.

For a clamping force of 40 lb, the maximum compressive stess is 501 psi and the maximum tensile stress is 235 psi, both of which are within the acceptable range. Note that these results can be scaled linearly for various clamping forces within the elastic range of the material.

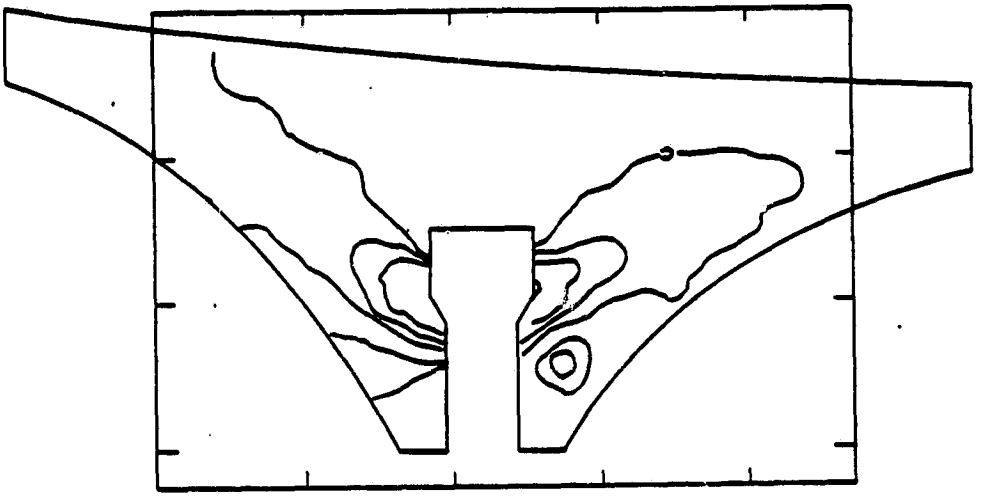

Figure 15. Stress profile of the normal stress, S_{11}.

Contour interval: 30 psi
Maximum normal stress: 129
Minimum normal stress: -81

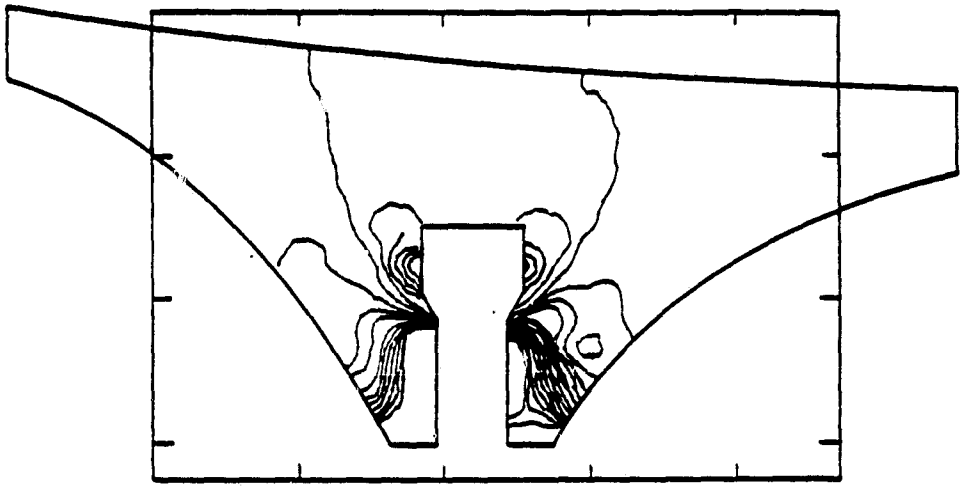

Figure 16. Stress profile of the normal stress, S_{22}.

Contour interval: 30 psi
Maximum compressive stress: -483 psi
Maximum tensile stress: +170 psi

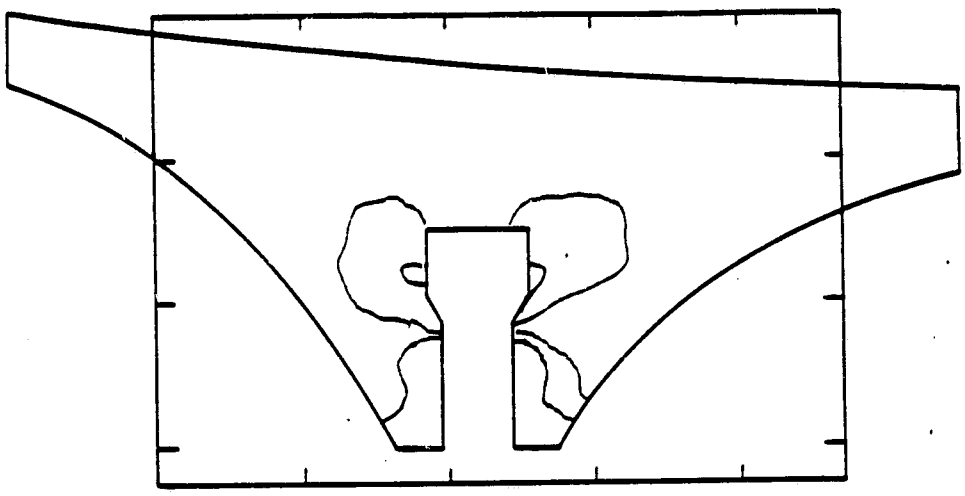

Figure 17. Stress profile of the normal stress, S_{33}.

Contour interval: 30 psi
Maximum compressive stress: -88 psi
Maximum tensile stress: +50 psi

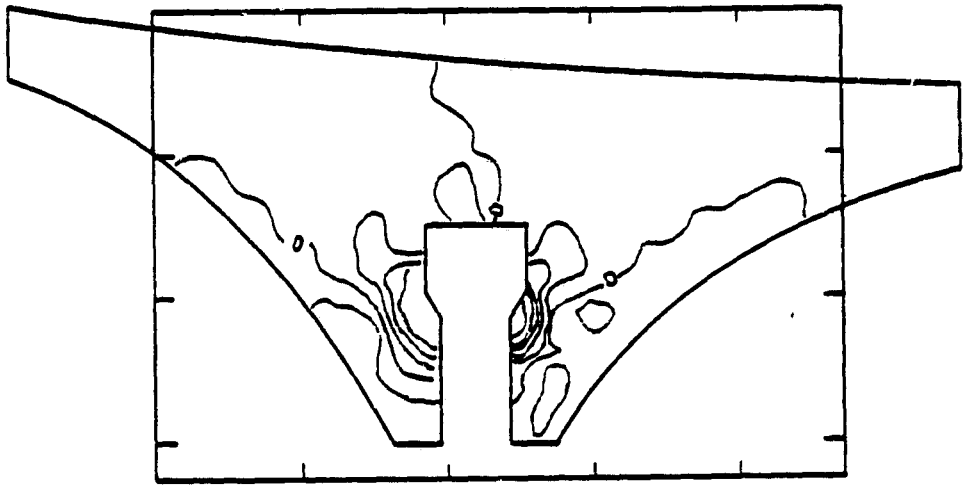

Figure 18. Stress profile for the shearing stress, S12.

Contour intervals: 30 psi
Maximum shearing stress: 210 psi

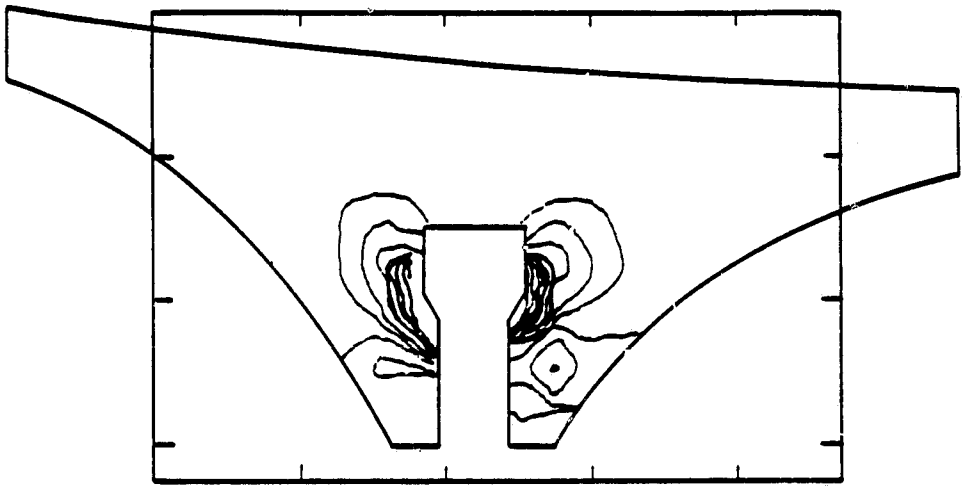

Figure 19. Stress profile of the major principal normal stress, S_{max}.

Contour interval: 30 psi
Maximum major principal stress: 236 psi
Minimum major principal stress: -63 psi

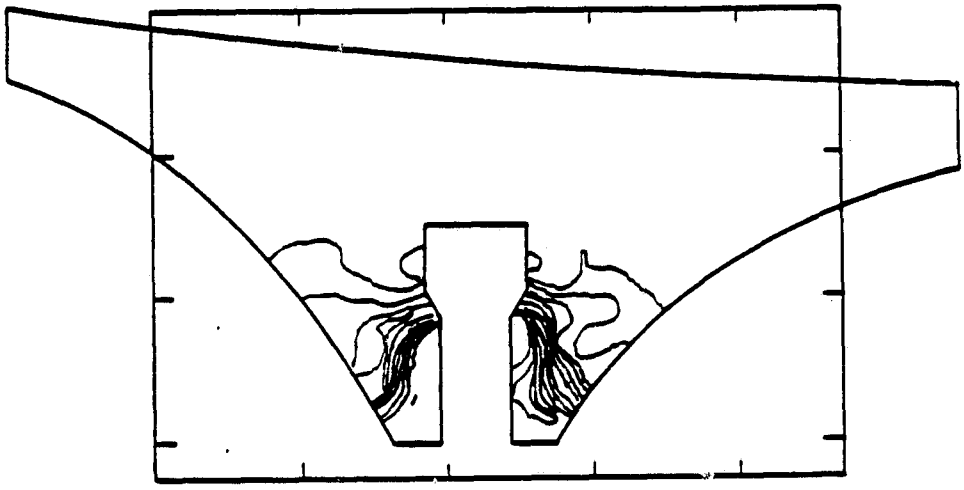

Figure 20. Stress profile of the minor principal normal stress, S_{min}.

Contour interval: 30 psi
Maximum minor principal stress: 28 psi
Minimum minor principal stress: -501 psi

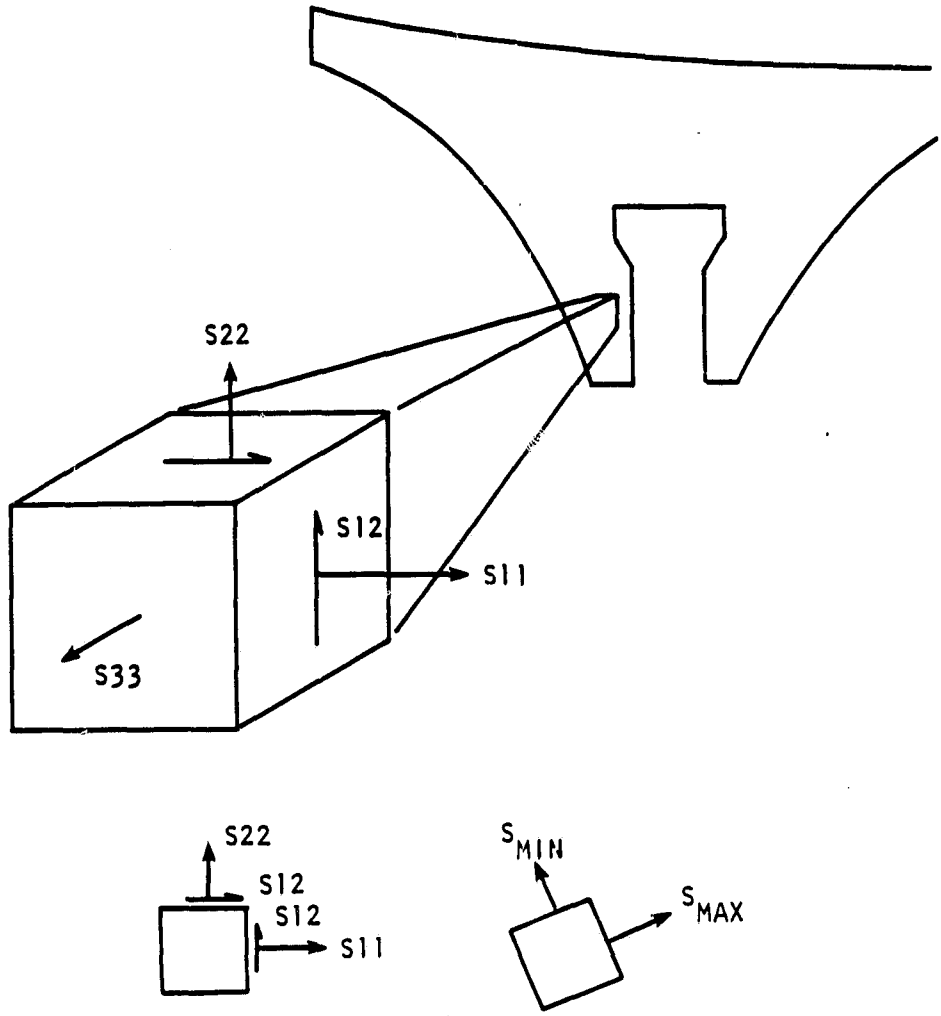

Figure 21. Definition of the stress components in axisymmetric model.

5. CONCLUSION

Figure 22 is a schematic of the proposed flexure design. The maximum normal and shear stress for this design is within the acceptable range. The effect of cool down as well as any mount-induced forces/moment are examined, and the contribution of any single error is limited to 2.5×10^{-6} in. RMS. The maximum compression and tensile stress inside the mirror due to a 40-lb clamping force are 501 psi and 235 psi, respectively.

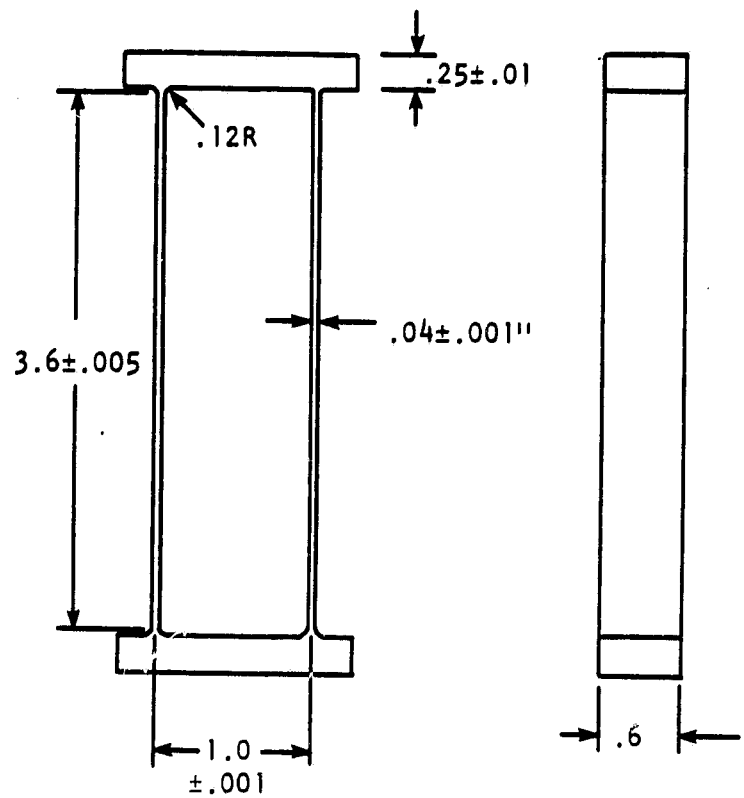

Figure 22. Proposed flexure design.

REFERENCES

1. G. A. Gabriele and K. M. Ragsdell, "OPTLIB: An Optimization Program Library," Purdue Research Foundation, 1979.

APPENDIX A

In this appendix an inclusive list of feasible design parameters with the calculated stress and RMS values is provided.

t (in.)	ℓ (in.)	x (in.)	b (in.)	Normal stress (psi) OG cool down plus mount error	Launch plus mount error	Emergency landing plus mount error	RMS (inch x 10^6) OG cool down	Radial tilt	Tang. tilt	Flex. error	Shear stress Launch plus mount error	Emergency landing plus mount error
.030	2.8	.6	.60	31625,	59320,	110388,	.05	.76	2.36	.07	2887,	5396,
.030	3.0	.6	.60	28015,	52473,	111096,	.04	.71	2.16	.06	2434,	5168,
.030	3.0	.8	.60	32952,	57409,	116033,	.04	.80	2.16	.08	2990,	5449,
.030	3.2	.6	.60	25842,	50263,	112441,	.03	.67	1.99	.05	2121,	4993,
.030	3.2	.8	.60	29365,	54586,	116764,	.03	.76	1.99	.06	2579,	5285,
.030	3.4	.6	.60	22541,	48545,	114277,	.03	.64	1.84	.04	1879,	4873,
.030	3.4	.8	.60	26377,	52361,	118093,	.03	.72	1.84	.05	2255,	5031,
.030	3.6	.6	.60	20468,	47214,	116581,	.02	.61	1.71	.03	1691,	4783,
.030	3.6	.8	.60	23848,	50606,	119893,	.02	.69	1.71	.05	2081,	4982,
.030	3.8	.6	.60	18684,	46193,	119034,	.02	.58	1.59	.03	1542,	4715,
.040	3.2	.4	.60	23314,	48162,	89978,	.03	.72	2.38	.06	1698,	3808,
.040	3.2	.8	.60	26524,	43372,	89188,	.08	.75	2.38	.09	1987,	3968,
.040	3.2	1.0	.60	29778,	46626,	92434,	.08	.83	2.38	.11	2329,	4143,
.040	3.2	1.2	.60	33867,	49916,	95723,	.08	.85	2.38	.13	2665,	4343,
.040	3.2	1.4	.60	36381,	53229,	99037,	.08	.87	2.38	.15	3007,	4562,
.040	3.2	1.6	.60	39713,	56561,	102368,	.08	.87	2.38	.17	3351,	4796,
.040	3.4	.4	.60	20995,	38419,	86895,	.07	.68	2.21	.05	1440,	3708,
.040	3.4	.8	.60	23824,	41248,	89724,	.07	.76	2.21	.07	1748,	3826,
.040	3.4	1.0	.60	26694,	44117,	92594,	.07	.79	2.21	.09	2017,	3960,
.040	3.4	1.2	.60	29597,	47021,	95497,	.07	.82	2.21	.11	2297,	4110,
.040	3.4	1.4	.60	32524,	49948,	98424,	.07	.83	2.21	.13	2579,	4275,
.040	3.4	1.6	.60	35468,	52892,	101368,	.07	.84	2.21	.16	2863,	4452,
.040	3.4	1.8	.60	38425,	55848,	104325,	.07	.85	2.21	.16	3149,	4641,
.040	3.6	.6	.60	19048,	37839,	88184,	.06	.69	2.06	.05	1319,	3636,
.040	3.6	.8	.60	21598,	39549,	90494,	.06	.72	2.06	.06	1586,	3725,
.040	3.6	1.0	.60	24098,	42097,	93242,	.06	.76	2.06	.08	1776,	3826,
.040	3.6	1.2	.60	26678,	44677,	95822,	.06	.79	2.06	.09	2008,	3948,
.040	3.6	1.4	.60	29281,	47280,	98425,	.06	.80	2.06	.11	2243,	4085,
.040	3.6	1.6	.60	31901,	49900,	101045,	.06	.81	2.06	.12	2479,	4230,
.040	3.6	1.8	.60	34533,	52532,	103677,	.06	.82	2.06	.14	2718,	4385,
.040	3.6	2.0	.60	37174,	55173,	106318,	.06	.82	2.06	.15	2957,	4499,
.040	3.8	.6	.60	17375,	35949,	89762,	.05	.62	1.93	.04	1200,	3581,
.040	3.8	.8	.60	19616,	38191,	92004,	.05	.70	1.93	.05	1393,	3640,
.040	3.8	1.0	.60	21892,	40467,	94280,	.05	.74	1.93	.06	1584,	3726,
.040	3.8	1.2	.60	24199,	42773,	96586,	.05	.76	1.93	.08	1778,	3813,
.040	3.8	1.4	.60	26528,	45102,	98916,	.05	.77	1.93	.09	1974,	3909,
.040	3.8	1.6	.60	28874,	47448,	101261,	.05	.78	1.93	.10	2173,	4013,
.040	3.8	1.8	.60	31231,	49806,	103619,	.05	.79	1.93	.12	2373,	4125,
.040	3.8	2.0	.60	33598,	52172,	105985,	.05	.80	1.93	.13	2575,	4245,
.040	4.0	.6	.60	15944,	35893,	91575,	.04	.68	1.81	.03	1113,	3530,
.040	4.0	.8	.60	17956,	37186,	93588,	.04	.67	1.81	.04	1278,	3591,
.040	4.0	1.0	.60	20001,	39198,	95632,	.04	.71	1.81	.05	1448,	3651,
.040	4.0	1.2	.60	22074,	41224,	97705,	.04	.73	1.81	.07	1593,	3718,
.040	4.0	1.4	.60	24169,	43319,	99801,	.04	.75	1.81	.08	1758,	3792,
.040	4.0	1.6	.60	26281,	45430,	101912,	.04	.76	1.81	.09	1926,	3872,
.040	4.0	1.8	.60	28404,	47554,	104035,	.04	.77	1.81	.10	2095,	3959,
.040	4.0	2.0	.60	30536,	49686,	106167,	.04	.77	1.81	.11	2266,	4053,
.050	3.6	.6	.60	18813,	32214,	72729,	.11	.68	2.36	.06	1096,	2943,
.050	3.6	.8	.60	20802,	34203,	74718,	.11	.75	2.36	.08	1278,	3015,
.050	3.6	1.0	.60	22832,	36233,	76748,	.11	.78	2.36	.09	1455,	3096,
.050	3.6	1.2	.60	24891,	38293,	78807,	.11	.80	2.36	.11	1639,	3187,
.050	3.6	1.4	.60	26972,	40373,	80888,	.11	.81	2.36	.13	1825,	3287,
.050	3.6	1.6	.60	29066,	42467,	82982,	.11	.82	2.36	.15	2013,	3395,
.050	3.6	1.8	.60	31171,	44572,	85087,	.11	.82	2.36	.17	2203,	3511,
.050	3.6	2.0	.60	33283,	46684,	87199,	.11	.83	2.36	.19	2394,	3634,
.050	3.8	.6	.60	17198,	31011,	73661,	.09	.66	2.22	.05	1008,	2894,
.050	3.8	.8	.60	18922,	32785,	75435,	.09	.72	2.22	.06	1148,	2951,
.050	3.8	1.0	.60	20734,	34596,	77247,	.09	.75	2.22	.08	1299,	3013,

				Normal stress (psi)			RMS (inch x 10^6)				Shear stress	
t (in.)	f (in.)	x (in.)	b (in.)	OG cool down plus mount error	Launch plus mount error	Emergency landing plus mount error	OG cool down	Radial tilt	Tang. tilt	Flex. error	Launch plus mount error	Emergency landing plus mount error
.050	3.0	1.2	.60	22575.	36437.	79088.	.09	.77	2.22	.10	1452.	3082.
.050	3.0	1.4	.60	24436.	38298.	80948.	.09	.78	2.22	.11	1608.	3159.
.050	3.0	1.6	.60	26311.	40173.	82823.	.09	.79	2.22	.13	1765.	3242.
.050	3.0	1.8	.60	28196.	42058.	84709.	.09	.80	2.22	.14	1925.	3332.
.050	3.0	2.0	.60	30088.	43951.	86601.	.09	.80	2.22	.16	2085.	3427.
.050	4.0	.6	.60	15719.	38043.	74829.	.08	.63	2.09	.04	924.	2859.
.050	4.0	.8	.60	17318.	31633.	76419.	.08	.69	2.09	.05	1007.	2901.
.050	4.0	1.0	.60	18936.	33249.	78045.	.08	.73	2.09	.07	1173.	2949.
.050	4.0	1.2	.60	20590.	34913.	79699.	.08	.75	2.09	.08	1302.	3003.
.050	4.0	1.4	.60	22263.	36587.	81373.	.08	.76	2.09	.10	1433.	3062.
.050	4.0	1.6	.60	23951.	38275.	83061.	.08	.77	2.09	.11	1565.	3127.
.050	4.0	1.8	.60	25649.	39972.	84758.	.08	.77	2.09	.12	1700.	3194.
.050	4.0	2.0	.60	27354.	41677.	86463.	.08	.78	2.09	.14	1836.	3271.
.060	2.4	.6	.40	40527.	56445.	106753.	.42	.92	1.84	.15	2460.	4211.
.060	2.6	.6	.40	34976.	51759.	106072.	.33	.86	1.82	.12	2030.	3956.
.060	2.6	.8	.40	38198.	54981.	109294.	.33	.93	1.82	.16	2470.	4200.
.060	2.8	.6	.40	30550.	48199.	106517.	.27	.88	1.64	.10	1731.	3785.
.060	2.8	.8	.40	33308.	50956.	109274.	.27	.88	1.64	.13	2079.	3957.
.060	2.8	1.0	.40	36117.	53766.	112084.	.27	.91	1.64	.16	2424.	4149.
.060	2.8	1.2	.40	38965.	56613.	114931.	.27	.93	1.64	.19	2760.	4360.
.060	3.0	.6	.40	26962.	45477.	107799.	.22	.76	1.49	.08	1501.	3668.
.060	3.0	.8	.40	29386.	47860.	110183.	.22	.83	1.49	.10	1781.	3792.
.060	3.0	1.0	.40	31778.	50292.	112615.	.22	.87	1.49	.13	2050.	3939.
.060	3.0	1.2	.40	34246.	52760.	115083.	.22	.89	1.49	.16	2339.	4082.
.060	3.0	1.4	.40	36739.	55254.	117576.	.22	.90	1.49	.18	2612.	4247.
.060	3.2	.6	.40	24811.	43391.	109719.	.18	.72	1.36	.06	1326.	3585.
.060	3.2	.8	.40	26898.	45478.	111797.	.18	.79	1.36	.09	1553.	3674.
.060	3.2	1.0	.40	28213.	47593.	113921.	.18	.83	1.36	.11	1778.	3777.
.060	3.2	1.2	.40	30371.	49751.	116079.	.18	.85	1.36	.13	2003.	3888.
.060	3.2	1.4	.40	32558.	51938.	118261.	.18	.87	1.36	.15	2229.	4010.
.060	3.4	.6	.40	21593.	41798.	112131.	.15	.68	1.25	.05	1192.	3525.
.060	3.4	.8	.40	23388.	43625.	113958.	.15	.76	1.25	.07	1378.	3592.
.060	3.4	1.0	.40	25248.	45493.	115826.	.15	.79	1.25	.09	1562.	3667.
.060	3.4	1.2	.40	27149.	47394.	117727.	.15	.82	1.25	.11	1747.	3750.
.060	3.4	1.4	.40	29074.	49319.	119652.	.15	.83	1.25	.13	1932.	3840.
.060	3.6	.6	.40	19483.	40593.	114930.	.13	.65	1.16	.05	1087.	3488.
.060	3.6	.8	.40	21099.	42210.	116547.	.13	.72	1.16	.06	1240.	3531.
.060	3.6	1.0	.40	22753.	43864.	118201.	.13	.76	1.16	.08	1392.	3587.
.060	3.6	1.2	.40	24440.	45550.	119888.	.13	.79	1.16	.09	1545.	3650.
.060	3.8	.6	.40	17721.	39697.	118039.	.11	.62	1.07	.04	1005.	3445.
.060	3.8	.6	.60	17482.	28478.	63795.	.16	.68	2.46	.06	846.	2439.
.060	3.8	.8	.40	19161.	41137.	119479.	.11	.70	1.07	.05	1132.	3485.
.060	3.8	.8	.60	18948.	29944.	65266.	.16	.75	2.46	.08	988.	2484.
.060	3.8	1.0	.60	20453.	31448.	66766.	.16	.76	2.46	.10	1112.	2536.
.060	3.8	1.2	.60	21984.	32980.	68297.	.16	.78	2.46	.12	1239.	2595.
.060	3.8	1.4	.60	23533.	34529.	69847.	.16	.79	2.46	.13	1368.	2659.
.060	3.8	1.6	.60	25095.	36091.	71408.	.16	.79	2.46	.15	1499.	2728.
.060	3.8	1.8	.60	26666.	37661.	72979.	.16	.80	2.46	.17	1631.	2803.
.060	3.8	2.0	.60	28242.	39238.	74556.	.16	.80	2.46	.19	1764.	2883.
.060	4.0	.6	.60	16084.	27384.	64481.	.14	.65	2.32	.05	799.	2484.
.060	4.0	.8	.60	17317.	28697.	65794.	.14	.71	2.32	.07	908.	2440.
.060	4.0	1.0	.60	18666.	30046.	67144.	.14	.74	2.32	.08	1004.	2481.
.060	4.0	1.2	.60	20042.	31422.	68519.	.14	.75	2.32	.10	1111.	2526.
.060	4.0	1.4	.60	21435.	32815.	69913.	.14	.76	2.32	.12	1219.	2575.
.060	4.0	1.6	.60	22840.	34221.	71318.	.14	.77	2.32	.13	1329.	2629.
.060	4.0	1.8	.60	24255.	35635.	72732.	.14	.78	2.32	.15	1441.	2688.
.060	4.0	2.0	.60	25675.	37055.	74153.	.14	.78	2.32	.16	1554.	2750.

APPENDIX B

In this appendix the effect of various combinations of mount error on the double arch mirror surface mounted on the proposed flexures is studied.

ORIGINAL PAGE IS
OF POOR QUALITY

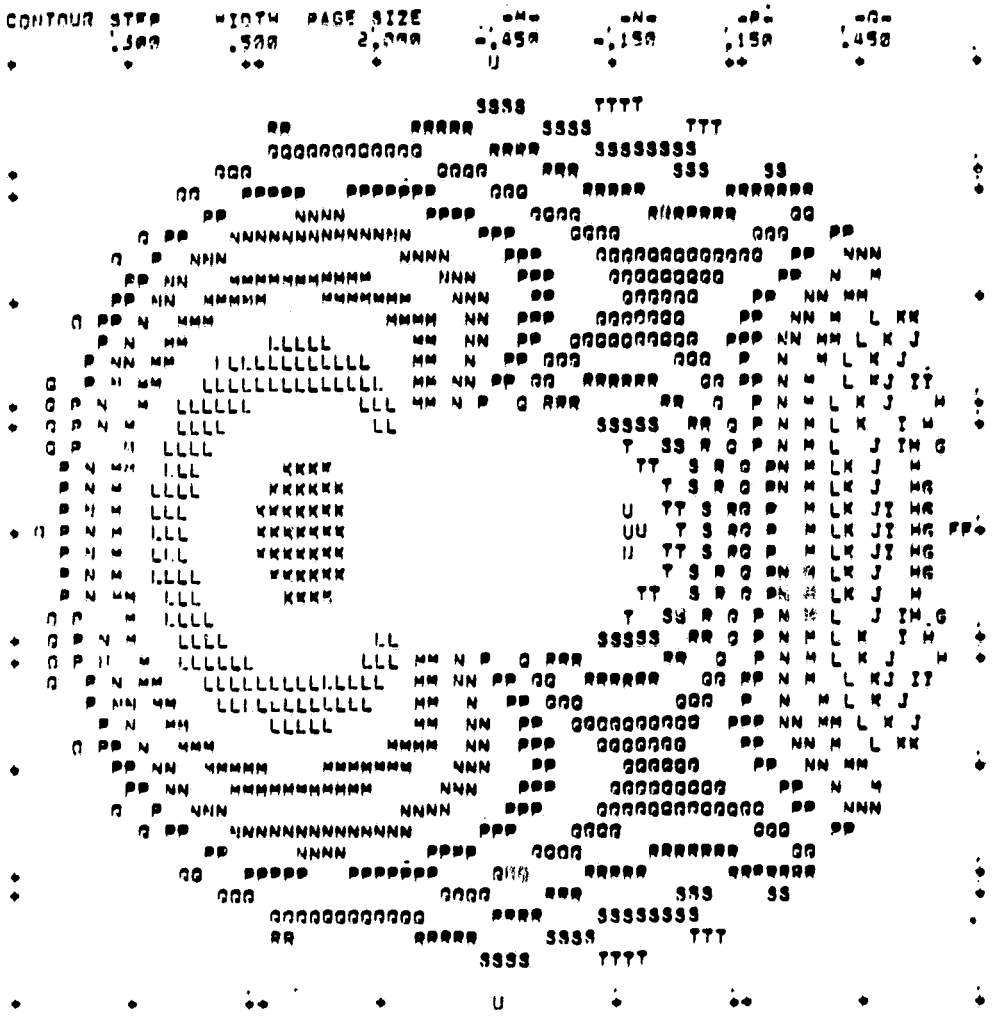

Figure A1. Cool down and radial tilt in one flexure location. Units = 10^6 in.

ZERNIKE POLYNOMIAL COEFFICIENTS

0.0000	0.0000	0.0000	-0.0000	4.7247	-0.0000	-0.0079	0.0642
-0.1147	0.7492	0.0000	-0.5639	0.0000	-0.0041	-0.0216	0.0000
0.2588	0.0025	-0.1873	0.0000	0.1739	-0.0000	-0.0026	0.0112
-0.0000	0.1775	-0.0000	-0.0794	0.0000	0.0720	-0.0000	-0.0546
0.0000	0.0018	-0.0038	0.0069				

RESIDUAL WAVEFRONT VARIATIONS OVER UNIFORM MESH

PTS	RMS	MAX	MIN	SPAN	VOLUM
464.	2.063	4.882	-4.682	9.564	13.818

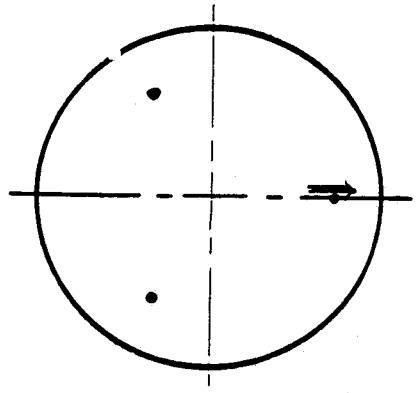

Figure A2. Cool down and tangential tilt in one flexure location. Units = 10^6 in.

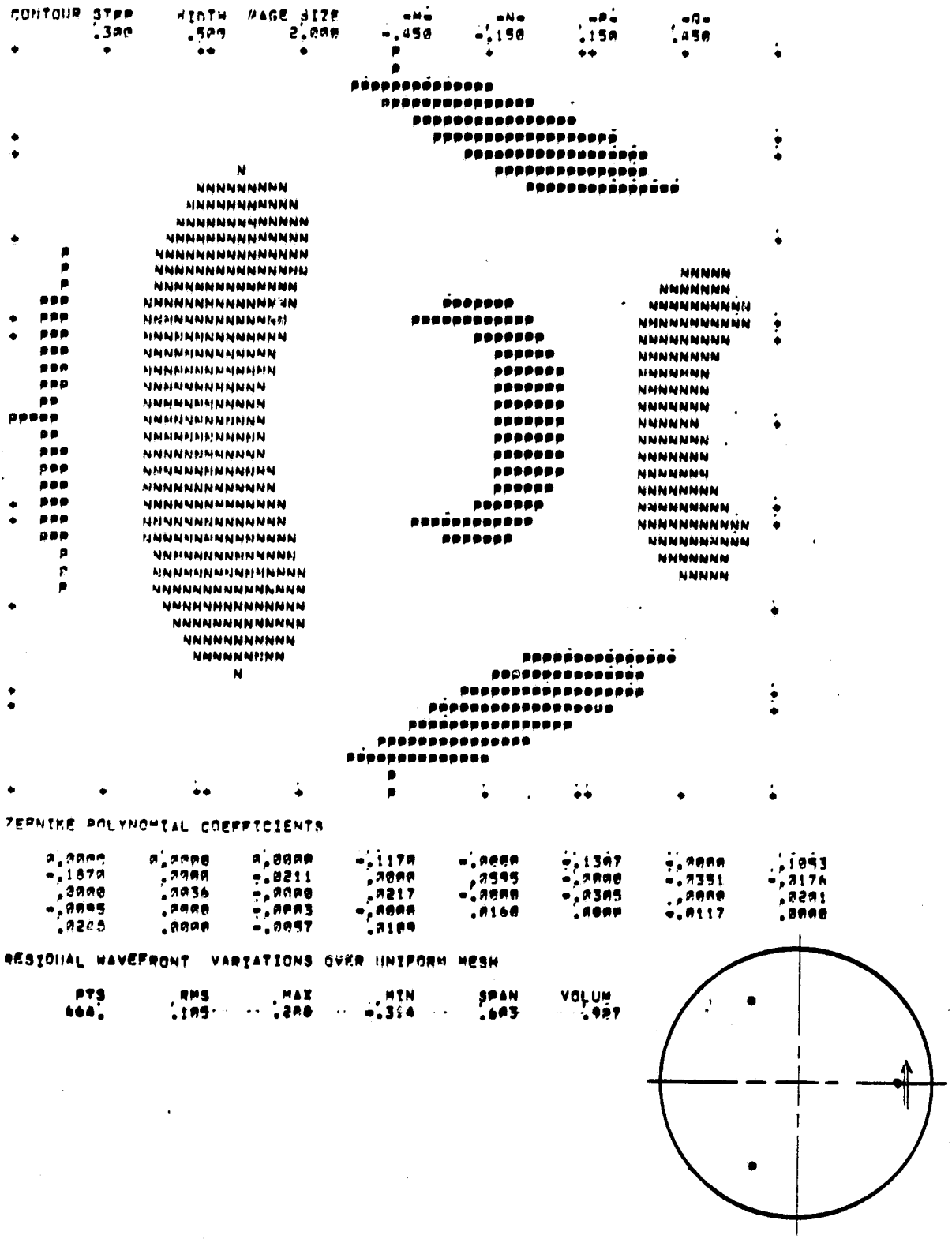

Figure A3. Cool down and flexure error in one flexure location. Units = 10^6 in.

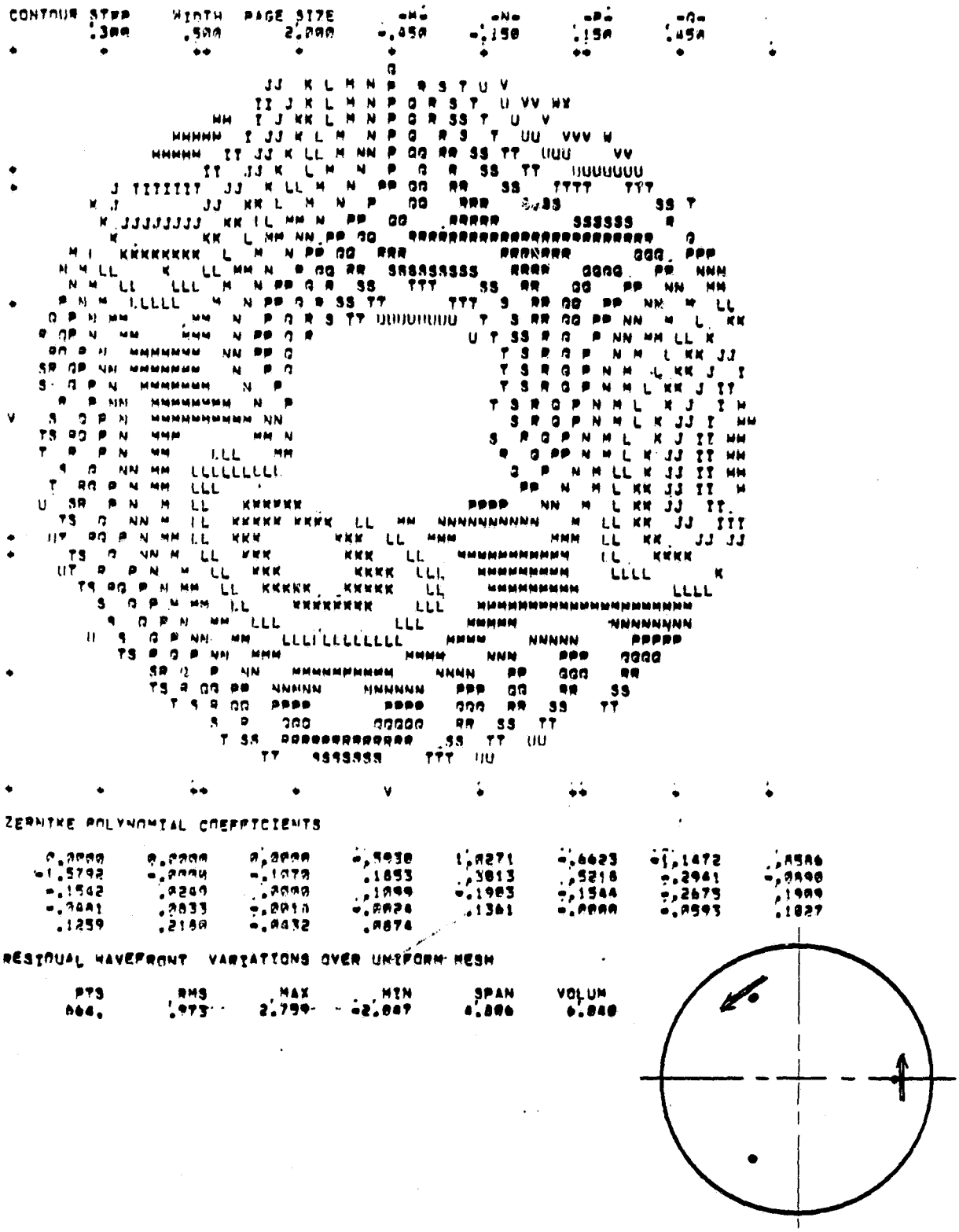

Figure A4. Cool down and radial tilt in two flexure locations. Units = 10^6 in.

Figure A5. Cool down and tangential tilt in two flexure locations. Units = 10^6 in.

ZERNIKE POLYNOMIAL COEFFICIENTS

0.0000	0.0000	0.0000	2.9857	-2.3623	-1.3178	.0848	.4624
-.8449	.7092	-.7033	.2819	.5990	-.0821	-.1579	-.0814
-.1294	.0137	-.1873	.3793	-.0869	-.3866	.0013	.1911
.0575	-.0897	.0660	.0397	.0729	.0720	-.1659	.0273
.2542	-.0009	-.0235	.0472				

RESIDUAL WAVEFRONT VARIATIONS OVER UNIFORM MESH

PTS	RMS	MAX	MIN	SPAN	VOLUM
644.	1.748	5.218	-3.125	8.335	9.222

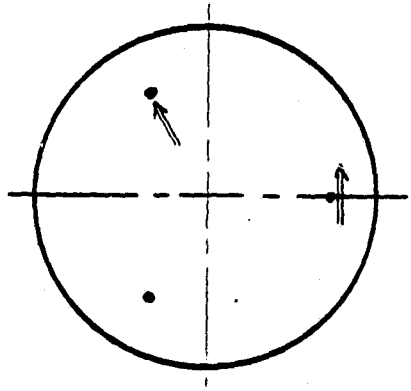

Figure A6. Cool down and radial and tangential tilt in two flexure locations. Units = 10^6 in.

ZERNIKE POLYNOMIAL COEFFICIENTS

0.0000	0.0000	0.0000	3.5612	3.3895	-.5857	-1.1511	.0060
-1.6543	1.4984	-.5840	-.0966	.2659	.0299	-.3885	-.3930
-.0252	.0268	-.3746	.2489	-.1034	-.1359	-.2688	.1974
.1107	.1720	.0675	-.0621	.1425	.1440	-.1003	.0794
.1110	.2189	-.0468	.0922				

RESIDUAL WAVEFRONT VARIATIONS OVER UNIFORM MESH

PTS	RMS	MAX	MIN	SPAN	VOLUM
664.	2.324	9.988	-6.336	12.316	18.698

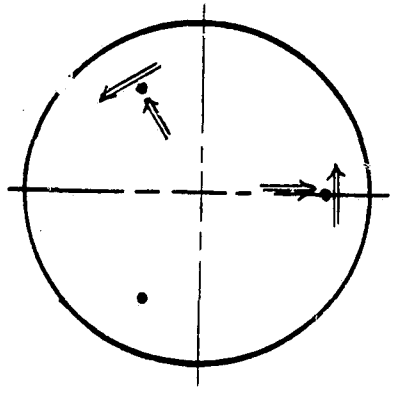

Figure A7. Cool down and radial and tangential tilt in two flexure locations. Units = 10^6 in.

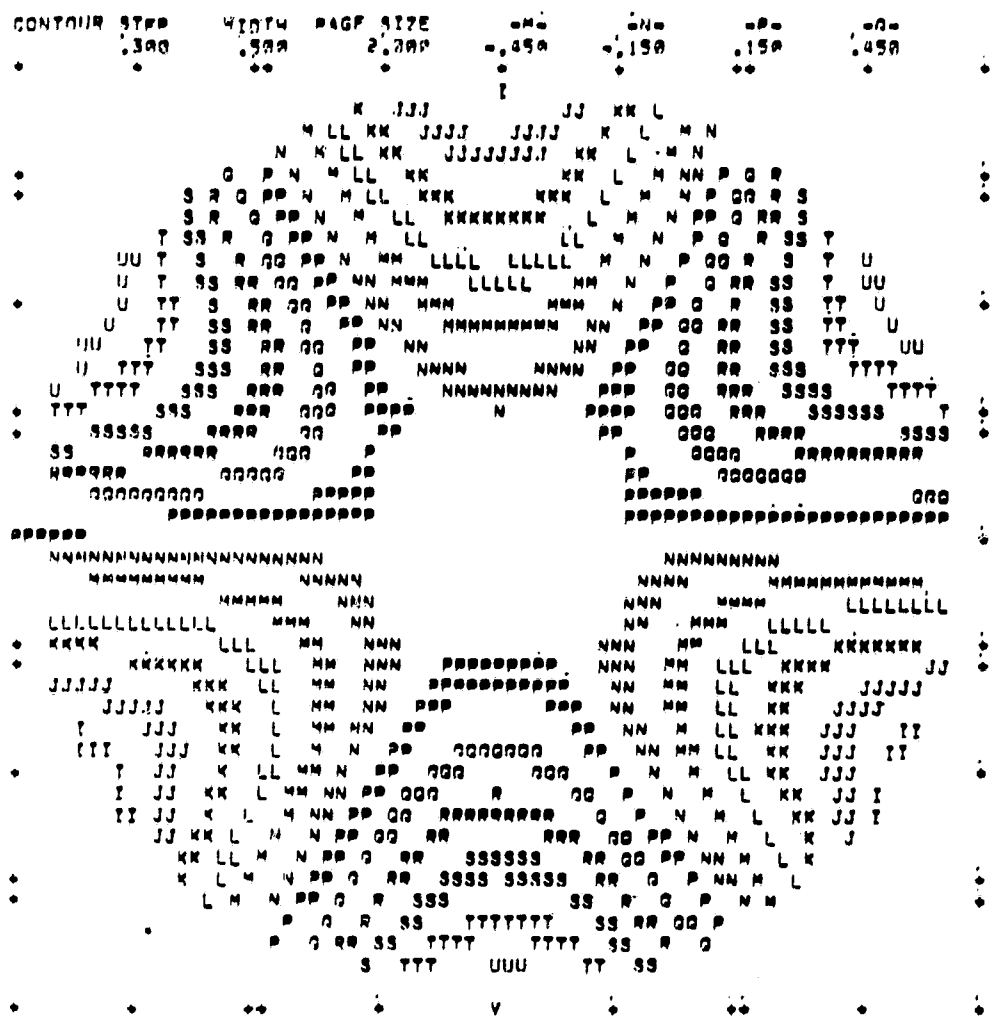

ZERNIKE POLYNOMIAL COEFFICIENTS

0.0000	0.0000	0.0000	-.0000	-.0000	-.0000	-.0000	.0662
-.1147	0.2475	.0000	.0000	.0000	.0000	-.0216	.0000
.0000	.0029	-.5629	.0000	-.0000	-.0000	-.0000	.0112
-.0000	.0000	-.0000	-.0000	.0098	.2168	-.0000	.0000
.0000	.0000	-.0038	.0069				

RESIDUAL WAVEFRONT VARIATIONS OVER UNIFORM MESH

PTS	RMS	MAX	MIN	SPAN	VOLUM
664.	.044	1.965	-1.938	3.903	5.424

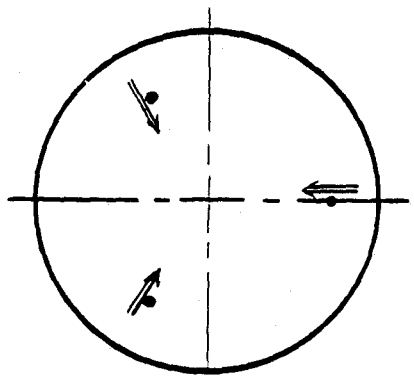

Figure A8. Cool down and tangential tilt in all three flexure locations. Units = 10^6 in.

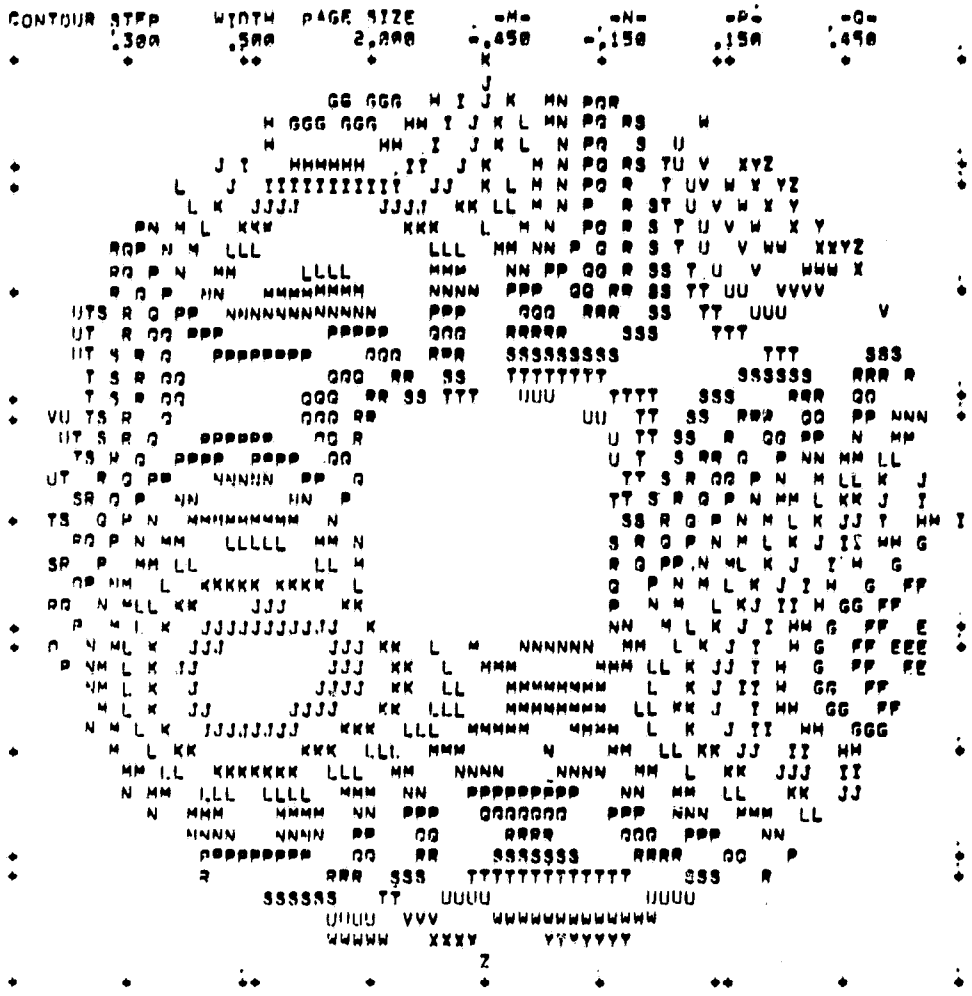

Figure A9. Cool down and radial and tangential tilt in all three locations. Units = 10^6 in.